THE ADDITION OF RETENTION DATA DERIVED FROM PEDO-TRANSFER FUNCTIONS IN ONE-STEP OUTFLOW OPTIMIZATION

A.F. Moene

RAPPORT 11

Oktober 1990

Vakgroep Hydrologie, Bodemnatuurkunde en Hydraulica
Nieuwe Kanaal 11, 6709 PA Wageningen

Formulas are powerful tools in science, having a high information density (Ω). They're real paper-savers. But the omission of the units of variables, renders formulas worthless obstacles. What sense does it make to multiply mice with elephants?

CONTENTS

LIST OF SYMBOLS

A	Surface area of soil core	cm^2
A	Coefficient (Saxton et al.)	kPa
B	Coefficient (Saxton et al.)	-
C	Water capacity	cm^{-1}
C_L	Percentage clay	%
D	Fractal dimension (Tyler and Wheatcraft)	-
D_T	Topological dimension	-
D_i	Fractal increment	-
F	Measure of line length (Tyler and Wheatcraft)	-
F	Cumulative particle-size distribution (Haverkamp and Parlange)	-
K	Hydraulic conductivity	$cm \cdot hr^{-1}$
K_s	Saturated hydraulic conductivity	$cm \cdot hr^{-1}$
L	x-coordinate at bottom of ceramic plate	cm
L	Length of a line (Tyler and Wheatcraft)	cm
N	Number of measuring units (Tyler and Wheatcraft)	-
N	Number of particles (Tyler and Wheatcraft)	-
OM	Organic matter content	%
Q_0	Measured cumulative outflow	cm^3
Q_c	Calculated cumulative outflow	cm^3
Q_{tot}	Total outflow during experiment	cm^3
R	Particle radius	cm
R	Equivalent pore radius (Haverkamp and Parlange)	cm
S	Relative saturation	-
SA	Percentage sand	%
SI	Percentage silt	%
V	Volume	cm^3
W	Mass fraction	-
b	Coefficient (Cosby et al.)	-
{b}	Set of Mualem-Van Genuchten parameters	
d	Particle diameter (Haverkamp and Parlange)	cm
d_g	Coefficient in function F (Haverkamp and Parlange)	cm
e	Void ratio	-
g	Gravitational acceleration	$m \cdot s^{-2}$

h	Pore length	cm
h	Pressure head	cm
h_0	Initial pressure head	cm
h_a	Applied pneumatic pressure head	cm
h_{ae}	Pressure head at air entry	cm
h_L	Initial pressure head below ceramic plate	cm
h_s	Saturation pressure head	cm
h_{std}	Starting pressure head at drying boundary curve (Haverkamp and Parlange)	cm
h_{we}	Pressure head at water entry (Haverkamp and Parlange)	cm
h^*	True length of fractal object (Tyler and Wheatcraft)	cm
l	Parameter in Mualem-Van Genuchten model	-
m	Parameter in Mualem-Van Genuchten model (=1 - 1/n)	-
m	Parameter in function F (Haverkamp and Parlange)	-
n	Parameter in Mualem-Van Genuchten model	-
n	Number of particles (Arya and Paris)	-
n	Parameter in function F (Haverkamp and Parlange)	-
r	Pore-radius	-
t	Time	hr
x	Coordinate	cm
Δx	Distance between successive nodes	cm
Ω	Information density	$bit \cdot m^{-2}$
α	Parameter in Mualem-Van Genuchten model	cm^{-1}
α	Coefficient (Arya and Paris)	-
α	Scaling factor	-
γ	Packing parameter (Haverkamp and Parlange)	-
ϵ	Measuring unit (Tyler and Wheatcraft)	cm
ϵ	Porosity	-
θ	Contact angle between water and capillary	°
θ	Water content	-
θ_{10}	Water content at 10 kPa	-
θ_{ae}	Water content at h_{ae} (Haverkamp and Parlange)	-
θ_d	Water content at drying curve (Haverkamp and Parlange)	-
θ_p	Water content at soil water pressure p	-

θ_r	Residual water content	-
θ_s	Saturated water content	-
θ_w	Water content at wetting curve (Haverkamp and Parlange)	cm
λ	Coefficient (Haverkamp and Parlange)	-
λ	Characteristic microscopic length	cm
μ	Parameter in limit function F (Haverkamp and Parlange)	-
ρ_b	Bulk density	$g \cdot cm^{-3}$
ρ_p	Particle density	$g \cdot cm^{-3}$
ρ_w	Water density	$g \cdot cm^{-3}$
σ	Surface tension	$g \cdot s^{-1}$

SUMMARY

For the quantitative description of soil hydrologic processes, the soil water retention curve and the hydraulic conductivity curve are indispensable. Most methods to determine these functions are time-consuming, expensive or both. Parameter estimation methods, like the one-step outflow method seem promising. In the one-step outflow method, parameters of the Mualem-Van Genuchten model, describing water retention and hydraulic conductivity, are evaluated by non-linear least squares fitting of predicted to observed outflow with time. Problems arise because a reasonable first guess is needed for the parameters and solutions suffer from non-uniqueness. The latter problem can be alleviated by the addition of independently measured or estimated retention data.
In this paper estimated retention data are used, derived from pedo-transfer functions, which relate texture and other easily measurable quantities to retention data. Pedo-transfer functions are either empirical, using regression equations between textural data and retention or parameters describing retention, or semi-empirical, relying on the shape-similarity between the retention curve and the cumulative particle-size distribution.
Textural and outflow data are available of 72 soil samples from the 'Hupselse Beek' catchment area. Data of an adjacent field are used for validation.
Four empirical pedo-transfer functions, of Gupta and Larson, Rawls and Brakensiek, Saxton et al. and Cosby et al., and three semi-empirical pedo-transfer functions, of Arya and Paris, Tyler and Wheatcraft and Haverkamp and Parlange, are tested against validation data. Average curves as well as the results of scaling are analyzed. The model of Tyler and Wheatcraft is chosen to be used for the combination with outflow data.
The inclusion of retention data in the one-step outflow optimization is accomplished by including one retention point in the object function of the optimization or by fixing the retention curve, optimizing only for the conductivity curve.
The inclusion of one retention point gives a reasonable average retention curve, but a too steep conductivity curve. The latter is also the result when the retention curve is fixed completely. Non-uniqueness is not reduced for both procedures when compared to optimization on outflow data only.
Due to inaccuracies in the outflow data, it is not possible to say whether these meagre results are attributable to errors in the pedo-transfer function, weaknesses in the one-step outflow method, or both.

PREFACE

My eyes are about as square a the monitor of a computer, but they have seen quite a many things.
Following a MSc-thesis in meteorology, in which I did a lot of field work, I had two questions when I asked Han Stricker for a subject for a second thesis. Firstly, I wanted to analyze data which other people had collected, because I knew already the despair connected to data-collection. Secondly, I wanted to go beneath the soil surface, having worked before on the layer of air above it. Han Stricker came up with the present subject, the combination of pedo-transfer data and outflow data to determine soil hydraulic properties. I was given the honourable task of trying to rescue a data set which was bound to be lost. At the start of this research I had only little knowledge about the theories concerning pedo-transfer functions and unsaturated flow. On my way, step by step, pieces began to fit together. If the jig-saw of soil science consists of 1000 pieces, I now may have found 10 pieces to fit together. So, there is no need for despair.
Again the best way of learning proved to be to work with people who know much more about the subject. Fortunately, they were available. Firstly I would like to thank Han Stricker for offering me the possibility to do this 3-months thesis. Whenever I had a question, I could drop in, even in his busiest moments, which are omnipresent. Also I am very obliged to Jos van Dam, who supplied me with computer programs, ideas, encouragements, and other practical matters. Paul Torfs I would like to thank for borrowing me his directory on the VAX-mainframe. I have used it exhaustively. Finally I am grateful to all these nameless people who collected the data I have worked with. I know the agony of collecting a reliable data set.
I would like to finish with some directions to the reader. Firstly, those not acquainted with soil physical nomenclature are directed to the glossary. Secondly, I am ashamed that I have to admit that I do not use SI units in this paper. I have followed the soil physical tradition of the use of grams, centimetres (if not inches !) and hours. However, I think that in the near future this should be prohibited.

Wageningen, october 1990

1. INTRODUCTION

The hydrological cycle comprises several subsystems, namely the systems of atmospheric water, surface water and subsurface water. Within and between these subsystems a variety of processes takes place, such as precipitation, evapo(transpi)ration, overland flow, runoff to streams and oceans, subsurface flow and groundwater flow (Chow et al., 1988). In order to make any quantitative statement about these processes one is in need of governing equations, describing the processes, and parameters, describing the properties of the subsystems and the processes.

In the present paper soil moisture transport in the unsaturated zone will be dealt with. More specifically the attention is directed to the determination of two soil hydraulic properties. These are the relationship of soil water content to soil water pressure (retention curve), $\theta(h)$, and the relationship of hydraulic conductivity to either soil water content or soil water pressure (which are interconnected by $\theta(h)$), $K(\theta)$ or $K(h)$ respectively. These two properties are indispensable for the modelling of unsaturated soil moisture flow, as can be seen from the one-dimensional, vertical Richards' equation (Kool et al.,1985):

$$C(h)\frac{\partial h}{\partial t} = \frac{\partial}{\partial x}[K(h)(\frac{\partial h}{\partial x} - 1)] \qquad [1.1]$$

with : h = pressure head (cm)
t = time (hr)
x = vertical coordinate (cm)
$K(h)$ = hydraulic conductivity ($cm \cdot hr^{-1}$)
$C(h) = \frac{\partial \theta(h)}{\partial h}$ = water capacity (cm^{-1})

The $\theta(h)$ and $K(h)$ relationships can be determined either directly or indirectly.

Direct laboratory determination of the $\theta(h)$ relationship involves the desorption of an initially saturated soil sample to a pre-specified pressure and the determination of its equilibrium water content. In the field the $\theta(h)$

relationship can be assessed directly by the in situ measurements of h, using a tensiometer, and of θ by neutron or gamma-ray attenuation (Arya and Paris, 1981). Because under field conditions periods of drying and wetting alternate, hysteresis causes the resulting retention curve to be a mixture of drying and wetting boundary or scanning curves. An overview of methods to determine θ(h) is given by Klute (1986).
Disadvantage of all methods is that they are rather time consuming, expensive or both.

Most direct methods to measure K(h) are based on the direct solution of the inverse problem. This means that either Darcy's equation or a simplified approximation of the one-dimensional unsaturated water flow equation (equation 1.1) is inverted and simplified in such a way that K can be expressed in terms of directly measurable variables. Both laboratory and field methods include steady-state as well as transient methods. Laboratory methods most frequently used are the crust method, sorptivity method, evaporation method and hot air method. Field methods are e.g. the infiltration gradient method and the instantaneous profile method. Klute and Dirksen (1986) give an overview of various laboratory methods to measure the K(h) relationship, whereas Green et al. (1986) review field methods.
Two major drawbacks can be distinguished. The first is the time consumptiveness because of the relatively restrictive initial and boundary conditions and (for some methods) the need for the achievement of some steady-state situation. Secondly, errors may be introduced as a result of the simplifications of the governing flow equations, necessary to allow their (semi-)analytic inversion (Van Genuchten, 1989).

At least some of the drawbacks of the methods to determine θ(h) or K(h), mentioned above, are alleviated by recently introduced parameter estimation methods. In these methods the direct flow problem can be formulated for any set of initial and boundary conditions (Van Genuchten, 1989). For the θ(h) and K(h) relationships a mathematical expression is used, containing a limited number of parameters. The flow problem is simulated, optimizing the parameters in the expressions of θ(h) and K(h), until the optimal fit between measured and simulated flow is found according to some object function (Kool et al., 1985a). An extra advantage of these methods is, that one is able to compute the accuracy of the results (Van Dam, pers. com., 1990).

An example of these parameter estimation methods is the one-step outflow method (Parker et al., 1985; Kool et al., 1985b). A recent modification is the multi-step outflow method (Van Dam et al., 1990)
Problems that may arise in the use of parameter estimation methods are non-uniqueness of the solution and the need for a reasonable first guess of the parameters.

A class of methods intermediate between 'direct' and 'indirect' comprises methods to determine K(h) from θ(h), using some pore size distribution model. These methods are based on the use of a mathematical expression to describe θ(h) which has some or all parameters in common with an expression describing K(h). These parameters can then be estimated from θ(h) data. The two most well-known formulations are those of Campbell (1974) and of Van Genuchten (1980).

Indirect methods are here referred to as pedo-transfer functions, a term stemming from quantitative land evaluation (Bouma, 1986). These methods are based on the relationships between soil hydraulic properties and other, usually easier to measure, properties, such as bulk density, organic matter content, particle size distribution. These methods can be classified as being either semi- or completely empirical.
The semi-empirical model for θ(h) of Arya and Paris (1979) is based on the similarity between the distribution of particle size and pore size (which is connected to θ(h)). The number of points of the θ(h) relationship which can be determined with this model depends on the number of particle size ranges in which the sample has been divided. The model of Haverkamp and Parlange (1986) is based on the same principle of shape similarity, but includes the effect of hysteresis and yields a curve rather than a set of points.
Empirical models are purely statistical relationships between soil hydraulic properties and basic soil properties. The models of Cosby et al. (1984), Saxton et al. (1986) and Vereecken (1989) estimate the parameters of mathematical expressions describing θ(h) and K(h). The models of Rawls and Brakensiek (1982), Rawls et al. (1982) and Gupta and Larson (1979) yield the soil water content at a limited number of soil water pressures.

In the framework of the research on the spatial variability of soil hydraulic properties, in 1988 a set of 72 soil samples was taken in the research catchment area 'Hupselse Beek'. In order to determine soil hydraulic properties one-

step outflow experiments were executed. However, it appeared that the optimization yielded unrealistic results. It is thought that this is a result of non-uniqueness in the parameter optimization procedure. According to Van Dam et al. (1990) a solution could be to add independent retention data to force the optimization into the right direction.
The aim of this research is to find out whether the addition of soil water retention data, derived from pedo-transfer functions, can improve the results of the parameter optimization from one-step outflow data.

In chapter 2 the various methods used in this research are reviewed and discussed, together with the data set and the way the aim stated above will be attained. In chapter 3 the results will be presented. Finally, in chapter 4 a discussion on the results will be given.

2. THEORY, MATERIAL AND METHODS

In this chapter firstly the one-step outflow method will be described (section 2.1). Next some remarks regarding the relationship between soil texture and the water retention curve will be given in section 2.2. In section 2.3 and 2.4 the empirical and semi-empirical the pedo-transfer functions will be treated respectively. Subsequently, spatial variability and the concept of scaling will be dealt with in section 2.5. Finally, the data sets used and the method of this research will be described in sections 2.6 and 2.7 respectively.

2.1 One-step outflow method

The one-step outflow method is one of the so-called inverse methods, which are used to determine both $\theta(h)$ and $K(h)$. Some flux related attribute of a flow system is measured. Starting with an initial guess for the parameters describing $\theta(h)$ and $K(h)$, the flow system is simulated. Based on the difference between the simulated and observed flow system, the parameter values are adjusted. The adjustment is repeated until the simulated flow process gives an optimal fit to the observed system. (Kool et al., 1985a). In the present case $\theta(h)$ and $K(h)$ are described by the Mualem-Van Genuchten model (Van Genuchten, 1980):

$$S = \frac{\theta - \theta_r}{\theta_s - \theta_r} \qquad [2.1.1]$$

$$S(h) = \frac{1}{[1 + |\alpha h|^n]^m} \qquad [2.1.2]$$

$$K(h) = K_s \cdot S^l [1 - (1 - S^{1/m})^m]^2 \qquad [2.1.3]$$

with :
- S = relative saturation (-)
- θ_s = saturated water content (-)
- θ_r = residual water content (-)
- α = fitting parameter (cm^{-1})
- n = fitting parameter (-)
- m = $1 - 1/n$ (-)
- K_s = saturated hydraulic conductivity ($cm.hr^{-1}$)
- l = fitting parameter (-)

Equations 2.1.2 and 2.1.3 have in common the parameters α and n and are linked by the theoretical pore size distribution model of Mualem (1976). Mualem assumed *l* to be 0.5, as did Van Genuchten (1980), but later (e.g. Wösten and Van Genuchten, 1988) he considered *l* to be an experimental variable. The parameter α is inversely related to the air entry pressure, while n is related to the slope of the retention curve (= water capacity C(h)). The latter is in turn connected to the width of the pore size distribution (Kool et al., 1985a). The effects of α and n on the shape of the retention curve work in the same direction. A higher value for α increases the slope of the retention curve as well as does an increase in n.

The flow process being evaluated in the one-step outflow method is the desorption of an, initially saturated, two-layer system of a soil sample and a ceramic plate to which an instantaneous pressure increment is applied. The cumulative outflow from the system is measured and used as input for the optimization procedure to find $\Theta(h)$ and K(h). The system of soil sample and ceramic plate is shown in figure 2.1.1.

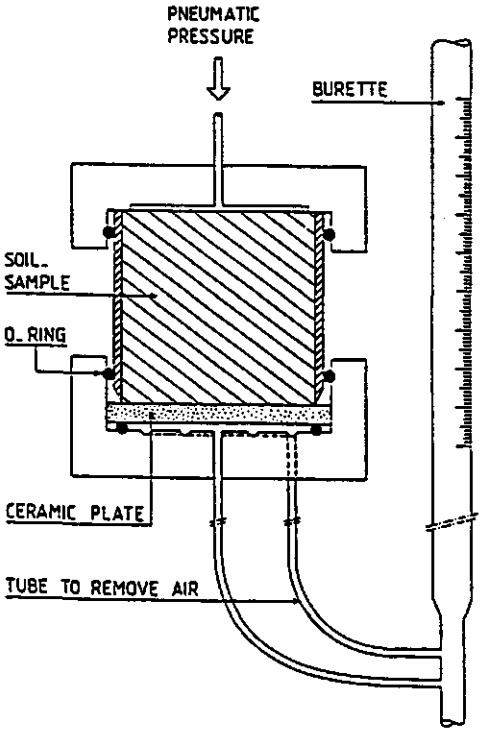

fig. 2.1.1. Cross section of Tempe-pressure cell (from: Van Dam et al.)

The system is mathematically described by the Richard's equation (equation 1.1), together with the following initial and boundary conditions and parameter set {b}:

$$h = h_0(x) \qquad t = 0 \qquad 0 \le x \le L \qquad [2.1.4]$$

$$\frac{\partial h}{\partial x} = 1 \qquad t > 0 \qquad x = 0 \qquad [2.1.5]$$

$$h = h_L - h_a \qquad t > 0 \qquad X = L \qquad [2.1.6]$$

$$\{b\} = \{\theta_s, \theta_r, \alpha, n, K_s, l\} \qquad [2.1.7]$$

with : x - vertical coordinate (cm) (x=0 at top of the soil core; x=L at bottom of ceramic plate)
h_0 - initial pressure head (cm)
h_a - applied pneumatic pressure head (cm)
h_L - initial pressure head below the ceramic plate (cm)
{b} - set of Mualem-Van Genuchten parameters

Cumulative outflow $Q_c(t)$ is calculated as :

$$Q_c(t) = A \sum_{x=0}^{L} [\theta(x,0) - \theta(x,t)] \cdot \Delta x \qquad [2.1.8]$$

with : A - surface area of soil core (cm^2)
Δx - distance between successive nodes (cm)

The object function E({b}) for the parameter estimation is of an ordinary least square form:

$$E(\{b\}) = [Q_0(t_i) - Q_c(t_i, \{b\})]^2 \qquad [2.1.9]$$

with : $Q_0(t_i)$ - measured cumulative outflow at time t_i (cm^3)

Besides, independently measured retention and conductivity data can be included in the object function. The squared deviations between measured and simulated outflow, retention and conductivity data can be given different weights in the

optimization.
Van Dam et al. (1990) and Kool et al. (1985a) have investigated the merits and problems of the one step outflow method.

With respect to the flow process itself the following remarks have to be made. Firstly, at the start of the process the flow is mainly determined by the ceramic plate, being the only region where a pressure gradient exists. Later on the lower part of the soil sample adjusts to the suction of the plate and begins to dominate the flow process. This means that the outcome of a parameter optimization reflects the hydraulic properties of the lower, say, 20 % of the sample, rather than a sample average.
Secondly, due to the large instantaneous pressure increment applied at the start of the experiment, the possibility of non-Darcian flow should be kept in mind. The Darcy equation, which is the basis of Richard's equation (eq. 1.1), is only valid under the assumption of stationarity and the mere absence of friction within the fluid. These restrictions follow from the derivation of the Darcy equation from the Navier-Stokes equations. In order to make some quantitative statement about this, dimensional analysis can be used (see appendix 3).

Sensitivity analysis showed that the optimization is not disturbed by small errors in burette readings and in the conductivity of the ceramic plate. The optimization is however rather sensitive to leakage (systematic error in outflow) and incomplete saturation of the sample at the start of the experiment. The latter problem can be circumvented by starting the experiment at some (known) suction.
The optimization is also influenced by the restraints put on the various parameters. Firstly, it is a mathematical necessity that $n > 1.1$. Further, it does not make sense to optimize both θ_s and θ_r because the outflow is determined by the difference between these two parameters. Van Dam et al. (1990) claim that l is necessary as a fitting parameter in order to make the description of K(h) flexible enough. However some boundaries (-0.5 and 1.5) should by used to avoid large deviations in the optimization.
Van Dam et al. (1990) showed that outflow data alone are not sufficient to yield unique results. Non-uniqueness can result both from the high correlation between parameters and from local minima in the response surface of the object function. According to Van Dam (pers. com., 1990) non-uniqueness of parameter

optimization results especially occurs for soils with extreme textures, viz. sandy and clayey soils.

Kool et al. (1985a) have investigated the effect of the choice of initial parameter values on the parameter optimization, related to the applied pressure increment and the total amount of outflow (Q_{tot}) during the experiment. They used artificial outflow data for two hypothetical soils ('sandy loam' and 'clay loam'). They optimized for α, n and θ_r, keeping θ_s, K_s and l constant. Problems arose when Q_{tot} was small compared to the equilibrium outflow ($Q(t_\infty)$) which would occur at $t \to \infty$. This problem can be circumvented by either increasing h_a, or increasing the duration of the experiment, or including $Q(t_\infty)$ in the optimization. The latter possibility does not imply that the simulation has to be extended ad infinitum. $Q(t_\infty)$ in fact only gives information on (θ_s - $\theta(h_a)$) and thus has the same effect on the optimization as the inclusion of an independently measured retention point $\theta(h_a)$. Q_{tot} can also be increased by increasing h_a, which has the additional advantage that the experimental range of h is increased.
Their overall conclusion is that accurate and unique estimates for $\theta(h)$ and $K(h)$ can be obtained from outflow data under some conditions. These are that $Q_{tot}/Q(t_\infty) > 0.5$, $Q(t_\infty)$ is included and the measurements of outflow and θ_s are rather accurate, and the measurement of K_s is accurate within 25 %. (Kool et al., 1985). Regarding the latter requirement it should be noted that such accuracy is hardly attainable, due to the probable occurrence of preferential stream channels. Besides, K_s is usually not representative for the conductivities at higher suctions and therefore the conductivity curve should not be fixed to K_s.

The parameter optimization can be carried out by the FORTRAN program ONESTP (Kool et al., 1985b), or the modification of this program, MULSTP by Van Dam.

2.2 Relationship between texture and the retention curve

The relationship between soil water pressure and soil water content depends on the complicated interaction between soil water and the soil matrix. That intricacy is due to the irregularity of the pore spaces and the dependence of forces between water and the matrix on temperature, the composition of the soil

water and the nature of the solid phase. Due to these complications a microscopic description of soil water phenomena is impossible and so the derivation of a water retention curve from first principles.
To shift the problem from a microscopic to a macroscopic problem the continuum concept has to be invoked (Bear and Bachmat, 1990). This means that soil water and the soil matrix are both assumed to be continuous and that properties (e.g. soil water tension, porosity, bulk density) of both media can be described by a volume average. This introduces the problem of the definition of a representative elementary volume (REV). The scale of this REV should be some orders of magnitude larger than the scale of the individual features constituting the 'continuum' but small enough to circumvent spatial variations of the averages of the properties. The problem in the application of the continuum concept for a soil is that there are at least two scales, a textural (related to soil particles) and a structural (related to aggregates). On the sub-aggregate scale the soil looks different from that on a super-aggregate scale. When the pore space is described, using particle size distribution, a 'textural pore space' is described. The soil water retention curve, however, is a expression of the (inseparable) combination of 'textural' and 'structural pore space' (Childs, 1969).
The existence of at least two scales in soils has also consequences for the size of the sample (100 cm^3 cylinder or lysimeter) of which e.g. soil hydraulic properties are measured.

One of the quantities which describes the soil matrix at a macroscopic level, disregarding the exact microscopic arrangement of particles and structural elements, is particle size distribution. A connection between soil texture and the soil water retention curve might be expected. The particle size distribution determines to some extent the distribution of the room between the particles. i.e. pore size distribution. A soil consisting of large particles presumably has larger pores than a fine textured soil. And, keeping in mind the equation of capillarity, relating water pressure to the radius of a capillary, the water retention curve is nothing but a relationship between pore radius and cumulative pore volume (Haverkamp and Parlange, 1986). This is however not a unique relationship due to hysteresis. Besides, Haverkamp and Parlange (1982) claim that only the wetting boundary of the retention curve can be derived from cumulative particle size distribution.

Methods to relate the water retention curve to soil texture are treated in sections 2.3 and 2.4. Limitation to these methods is the limited amount of information contained in texture data. Factors, other than soil texture, influencing the water retention curve are soil structure (cracks, swelling, aggregation), packing of soil particles within aggregates and composition of the solid phase (clay minerals, organic matter). To circumvent these limitations partly, some of the described methods use additional data such as organic matter content, bulk density or saturated water content.

2.3 Empirical pedo-transfer functions

In this section four empirical methods to derive retention data from texture data will be dealt with. These are the methods of Gupta and Larson (1979), Rawls and Brakensiek (1982), Saxton et al. (1986) and Cosby et al. (1984).

2.3.1 Gupta and Larson

Gupta and Larson (1979) developed statistical relationships predicting soil water retention at 12 soil water pressures, viz. -0.04, -0.07, -0.10, -0.20, -0.33, -0.60, -1.0, -2.0, -4.0, -7.0, -10.0, -15.0 bar. These relationships are based on percentages sand, silt, clay and organic matter and bulk density. The retention and texture data were obtained from 43 soil materials, of which 40 were artificially packed cores. The artificial soil samples were composed of dried soil material from ten locations in the United States plus a dredged sediment. Retention data were smoothed and the water content values used in the regression analysis were taken from the smoothed curve.
Regression coefficients were determined for the following equation, relating water content to texture data:

$$\theta_p = a \cdot SA + b \cdot SI + c \cdot CL + d \cdot OM + e \cdot \rho_b \qquad [2.3.1]$$

with : θ_p = water content at pressure head p (-)
SA = percentage sand (%)
SI = percentage silt (%)
CL = percentage clay (%)
OM = organic matter content (%)

ρ_b = bulk density ($g \cdot cm^{-3}$)

a, b, c, d = regression coefficients (-)

e = regression coefficient ($cm^3 \cdot g^{-1}$)

Regression coefficients can be found in table 2.3.1.

Table 2.3.1. Regression and correlation coefficients for prediction of soil water content at specific matric potentials (Gupta and Larson, 1979)

Matric potential	Regression coefficients					Correlation coeff.
	a x 10^3	b x 10^3	c x 10^3	d x 10^3	e x 10^2	
bar	-	-	-	-	$cm^3 \cdot g^{-1}$	-
-0.04	7.053	10.242	10.070	6.333	-32.120	0.950
-0.07	5.678	9.228	9.135	6.103	-26.960	0.959
-0.10	5.018	8.548	8.833	4.966	-24.230	0.961
-0.20	3.890	7.066	8.408	2.817	-18.780	0.962
-0.33	3.075	5.886	8.039	2.208	-14.340	0.962
-0.60	2.181	4.557	7.557	2.191	-9.276	0.964
-1.0	1.563	3.620	7.154	2.388	-5.759	0.966
-2.0	0.932	2.643	6.636	2.717	-2.214	0.967
-4.0	0.483	1.943	6.129	2.925	-0.204	0.962
-7.0	0.214	1.538	5.908	2.855	1.530	0.954
-10.0	0.076	1.334	5.802	2.653	2.145	0.951
-15.0	-0.059	1.142	5.766	2.228	2.671	0.947

2.3.2 Rawls and Brakensiek

The approach of Rawls and Brakensiek (1982) is quite similar to that of Gupta and Larson (1979), but the first made use of natural soils instead of artificial soil samples. Using a U.S. data base of 500 soil profiles, comprising 2543 soil horizons, Rawls and Brakensiek developed regression equations to predict retention data from texture. They fitted the Brooks and Corey equation (Brooks and Corey, 1964; see also section 2.3.4) to the measured retention data. Subsequently, water contents were calculated for 12 pressure heads, using these curves. The pressure heads are the same as those used by Gupta and Larson (see 2.3.1).

Three levels of regression equations were developed. At the first level only percentages sand, silt, clay and organic matter and bulk density were used. At the second level the water retention at -15.0 bar was added and at the third

level the retention at -0.33 bar. Because in this research only textural data are available, the second and third level are of no use. When available, especially the retention at -0.33 bar might give much information. The regression equation for the first level reads as follows:

$$\theta_p = a + b \cdot SA + c \cdot SI + d \cdot CL + e \cdot OM + f \cdot \rho_b \qquad [2.3.2]$$

with : a, b, c, d, e = regression coefficients (-)
f = regression coefficient ($cm^3 \cdot g^{-1}$)

The regression coefficients are summarized in table 2.3.2.

Table 2.3.2. Regression and correlation coefficients for prediction of soil water content at specific matric potentials (Rawls and Brakensiek, 1982)

Water pressure	Regression coefficients						Correlation coeff.
	a	b	c	d	e	f	
bar	-	-	-	-	-	$cm^3 \cdot g^{-1}$	-
-0.04	0.7899	-0.0037			0.0100		0.58
-0.07	0.7135	-0.0030		0.0017		-0.1963	0.74
-0.10	0.4118	-0.0030		0.0023	0.0317		0.81
-0.20	0.3121	-0.0024		0.0032	0.0314		0.86
-0.33	0.2576	-0.0020		0.0036	0.0299		0.87
-0.60	0.2065	-0.0016		0.0040	0.0275		0.87
-1.0	0.0349		0.0014	0.0055	0.0251		0.87
-2.0	0.0281		0.0011		0.0220		0.86
-4.0	0.0238		0.0008	0.0052	0.0190		0.84
-7.0	0.0216		0.0006	0.0050	0.0167		0.81
-10.0	0.0205		0.0005	0.0049	0.0154		0.81
-15.0	0.0260			0.0050	0.0158		0.80

2.3.3 Saxton, Rawls, Roberger and Papendick

Saxton et al. (1986) observed that the water retention curve can not be described, from saturation to wilting point, by an exponential equation, nor by any other first or second order equation, because of the double inflection point in the curve. Therefore, they proposed a description which consists of three sections (see fig 2.3.1).

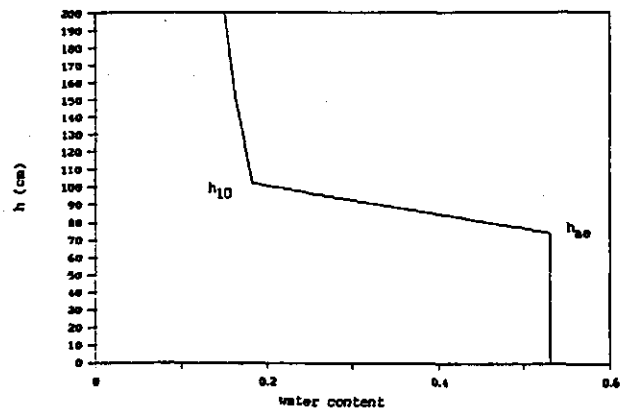

fig. 2.3.1. Retention curve divided into three sections according to Saxton et al. (1986)

For soil water pressures ranging from 10 to 1500 kPa an exponential function is applied, equation 2.3.3a (to convert from kPa to cm, multiply with 10.1936). Between 10 kPa and the water pressure at air entry, h_{ae}, a linear relationship gives a good approximation (equation 2.3.3b). Between h_{ae} and saturation water content is supposed to be constant (equation 2.3.3c):

$$h = A \cdot \theta^{B} \qquad 10 < h < 1500 \text{ kPa} \qquad [2.3.3a]$$

$$h = 10 - \frac{\theta - \theta_{10}}{\theta_s - \theta_{10}}(10 - h_{ae}) \qquad h_{ae} < h < 10 \text{ kPa} \qquad [2.3.3b]$$

$$\theta = \theta_s \qquad 0 < h < h_{ae} \qquad [2.3.3c]$$

with : A = coefficient (kPa)
B = coefficient (-)
θ_{10} = water content at h = 10 kPa (-)
h_{ae} = water potential at air entry (kPa)

In order to establish regression equations to estimate the coefficients in the above mentioned equations, hypothetic soils were generated. 55 soil textures were generated by dividing the USDA soil texture triangle into grids of 10 % sand and 10 % clay increments. Organic matter content was held constant at 0.66 %.
Artificial water retention data were generated using the regression equation of Rawls et al. (1982), predicting water content at 10 values of pressure head, using percentages sand, silt, clay and organic matter as input data.

Table 2.3.3. Summary of regression equations (Saxton et al., 1986)

Equation		Coefficient
A	$= \exp [a + b \cdot CL + c \cdot SA^2 + d \cdot SA^2 \cdot CL] \cdot 100.0$	a, b, c, d
B	$= e + f \cdot CL^2 + g \cdot SA^2 + g \cdot SA^2 \cdot CL$	e, f, g
θ_{10}	$= (10/A)^{1/B}$	
h_{ae}	$= 10.(m + n \cdot \theta_s)$	m, n
θ_s	$= h + j \cdot SA + {}^{10}\log(CL)$	h, j, k

Because of the limited range of textures in the original data of Rawls et al. (1982), hypothetic soils with >60 % clay, <5 % sand or <5 % clay were omitted. The resulting regression equations can be found in table 2.3.3, the regression coefficients in table 2.3.4.

Table 2.3.4. Regression coefficients (Saxton et al., 1986)

Coefficient	Value	Coefficient	Value
a	-4.396	g	$-3.484 \cdot 10^{-5}$
b	-0.0715	h	0.332
c	$-4.880 \cdot 10^{-4}$	j	$-7.521 \cdot 10^{-4}$
d	$-4.285 \cdot 10^{-5}$	k	0.1276
e	-3.140	m	-0.108
f	$-2.22 \cdot 10^{-3}$	n	0.341

2.3.4 Cosby, Hornberger, Clapp and Ginn

Cosby et al. (1984) described the water retention curve with a modification of the Brook and Corey (1964) equation (eq. 2.3.6), setting θ_r to zero (eq. 2.-3.7):

$$h = h_s\left(\frac{\theta - \theta_r}{\theta_s - \theta_r}\right)^b \qquad [2.3.6]$$

$$h = h_s\left(\frac{\theta}{\theta_s}\right)^b \qquad [2.3.7]$$

with : hs = saturation pressure head (cm)
b = coefficient (-)

The parameter h_s is comparable to the air entry pressure h_{ae}, but h_s in this case was used as a fitting parameter instead of a physical parameter. Cosby et al. took θ_s as a measured quantity and h_s and b were estimated by fitting equation 2.3.7 to the retention data. This was done for 1448 samples form U.S. soils, comprising the entire textural spectrum. Apart from texture, other descriptors of the samples were available, such as horizon, consistency, structural size and form, roots, topography, drainage and land use. Using one and two way analysis of variance they showed that texture was the most significant descriptor for both b and $\log(h_s)$.

In the data set texture was given as a textural class (according to the 12 textural classes in the USDA textural triangle), not as percentages sand, silt and clay. In order to develop regression equations between texture and the parameters h_s and b, percentages were obtained from the midpoint values of each textural class. Regression equations were also developed for $\log(K_s)$, θ_s and the standard deviations of b, h_s, θ_s and $\log(K_s)$. Regression equations are of the following form:

$$x = a + b \cdot SA + c \cdot SI + d \cdot CL \qquad [2.3.8]$$

with : x = b (-), h_s (cm), θ_s (-), $\log(K_s)$ ($\log(\text{inch.hr}^{-1})$), $\sigma(b)$ (-), $\sigma(h_s)$ (cm), $\sigma(\theta_s)$ (-), $\sigma(\log(K_s))$ ($\log(\text{inch.hr}^{-1})$)

a, b, c, d = coefficients ([x])

Table 2.3.5. Regression and correlation coefficients (Cosby et al., 1984)

Parameter		Regression coefficient				Correlation Coeff.
Name	Units [x]	a	b	c	d	
		[x]	[x]	[x]	[x]	-
b	-	-3.10	0.003		-0.1570	0.966
$\log(h_s)$	log(cm)	1.54	-0.0095	0.0063		0.850
$\log(K_s)$	$\log(\text{in}\cdot\text{hr}^{-1})$	-0.60	0.0126		-0.0064	0.872
θ_s	%	50.5	-0.142		-0.037	0.785
$\sigma(b)$	-	0.92		0.0144	0.0492	0.584
$\sigma(\log(h_s))$	log(cm)	0.72		-0.0026	0.0012	0.111
$\sigma(\log(K_s))$	$\log(\text{in}\cdot\text{hr}^{-1})$	0.43		0.0032	0.0011	0.403
$\sigma(\theta_s)$	%	8.23	-0.0070		-0.0805	0.574

The regression coefficients can be found in table 2.3.5. One remark has to be made with respect to parameter b. From physical considerations it is clear that b should be negative, because θ decreases as h increases. According to Cosby et al. (1984), however, b is positive. This error is corrected by multiplying all regression coefficients for b with -1.

2.4 Semi-empirical pedo-transfer functions

In this section three pedo-transfer functions will be described which are a combination of empiricism and physical considerations. These are the model of Arya and Paris (1981), the modification of this model by Tyler and Wheatcraft (1989) and the model of Haverkamp and Parlange (1986).

2.4.1 Arya and Paris

The model of Arya and Paris (1981) is based on the observation that there is an obvious similarity in shape between the water retention curve and the cumulative particle size distribution. The retention curve is in fact a pore size distribution curve (see section 2.2).

The cumulative particle size distribution is divided into n fractions (usually the same fractions as were used for the textural analysis). The particles of each fraction are thought to be assembled in a discrete domain with the same void ratio (ratio between pore volume and solid mass volume) as the undisturbed sample, where the void ratio is defined as:

$$e = (\rho_p - \rho_b)/\rho_b \qquad [2.4.1]$$

with : e = void ratio (-)
ρ_b = bulk density ($g \cdot cm^{-3}$)
ρ_p = particle density ($g \cdot cm^{-3}$)

The pore volume associated with each size fraction can then be computed as:

$$V_{v,i} = (W_i/\rho_p)\cdot e \qquad [2.4.2]$$

with : $V_{v,i}$ - specific pore volume associated with particles in fraction i ($cm^3.g^{-1}$)

W_i - mass fraction in particle size range i (-)

The pore volumes generated by each size fraction are successively filled with water, starting with the pores associated with the smallest particles. The water content related to each particle size fraction is computed as:

$$\theta_{v,i} = \sum_{j=1}^{j=i} V_{v,j}/V_b \qquad [2.4.3]$$

with : V_b - specific bulk volume = $1/\rho_b$ ($cm^3\cdot g^{-1}$)

The average volumetric water content corresponding to the midpoint of a given particle size fraction is approximately given by:

$$\theta^*_{v,i} = (\theta_{v,i} + \theta_{v,i+1})/2 \qquad [2.4.4]$$

with : $\theta^*_{v,i}$ - average volumetric water content in pore volume for which largest pore relates to midpoint of i-th particle size fraction (-)

Now the θ-coordinates of the points of the retention curve are determined. Subsequently the h-coordinates need to be assessed. h is related to the pore radius by the equation of capillarity, so that the problem is shifted to the determination of a representative pore radius for each particle size fraction. In order to establish a relationship between particle size and pore radius, two assumptions have to be made. Firstly, it is assumed that the solid volume in any fraction can be approximated as that of spheres with a uniform size, defined by the mean particle radius for that fraction. Secondly, it is assumed that the volume of the pores in each domain can be approximated as that of cylindrical capillary tubes with a uniform size, whose radii are related to the mean particle radius for that fraction.
With these assumptions, the particle and pore volumes in each particle size fraction can be represented respectively as:

$$V_{p,i} = n_i 4\pi R_i^3/3 = W_i/\rho_b \qquad [2.4.5]$$

$$V_{v,i} = \pi r_i^2 h_i = (W_i/\rho_p)\cdot e \qquad [2.4.6]$$

with : $V_{p,i}$ = specific solid volume in range i ($cm^3 \cdot g^{-1}$)
R_i = mean particle radius of range i (cm)
n_i = number of particles in range i (-)
r_i = mean pore radius related to range i (cm)
h_i = pore length of pores related to range i (cm)

Combining equations 2.4.5 and 2.4.6 gives:

$$r_i^2/R_i^3 = 4n_i e/3h_i \qquad [2.4.7]$$

The pore length h_i is approximated as the number of particles that lie along the pore path times the length contributed by each particle. In a cubic, closely packed assemblage of uniform spherical particles h_i would be $n_i 2R_i$. In natural soils, however, pore length will depend on actual soil particle shapes, size and orientation. The contribution of each particle to pore length will be greater than its diameter:

$$h_i = n_i^{\alpha} 2R_i \qquad [2.4.8]$$

with : α = empirical coefficient (-)

Pore radius can then be approximated as:

$$r_i = R_i[4e\cdot n_i^{(1-\alpha)/6}]^{1/2} \qquad [2.4.9]$$

Arya and Paris found α to be 1.38 on the average (ranging from 1.31 to 1.43) for fractions with a mean particle radius up to about 100 μm. For particles with larger radii α seems to drop sharply, but because of the scarce data in that size range, Arya and Paris decided to fix α at a value of 1.38.

When for each particle size fraction r_i has been calculated, soil water pressure can easily be obtained using the equation of capillarity:

$$h_i = 2\sigma \cdot \cos(\theta)/\rho_w \cdot g \cdot r_i \qquad [2.4.10]$$

with : θ - contact angle between water surface and capillary (°)
σ - surface tension of water ($g \cdot s^{-2}$ or 10^{-5}N/cm)
g - gravitational acceleration ($m \cdot s^{-2}$)
ρ_w - density of water ($kg \cdot m^{-3}$)

Although in reality θ depends on organic matter content, Arya and Paris set it to zero, which is only valid for an absolutely clean capillary. ρ_w and σ were held constant, while in reality they are temperature dependent.

Haverkamp and Parlange (1982) pointed out in their comment that the model of Arya and Paris does not take into account air entrapment, so that near saturation water content will be overestimated. Haverkamp and Parlange also stated that particle size distribution data can only be used for the determination of the wetting boundary curve. Finally they argued that the relation between pore and particle radii (eq. 2.4.8) is not uniquely defined as it depends on the way n_i is chosen. Having the same average particle radius, the width of the range of radii affects n_i. Arya and Paris (1982) showed in their reply that a drastic variation in n_i only has minor effects on the pore size.

2.4.2 Tyler and Wheatcraft

Tyler and Wheatcraft (1989) reduced the empiricism in the model of Arya and Paris (1981) (described in the previous section) by showing the physical significance of the empirical factor α, assumed to be constant at 1.38 by Arya and Paris. For this they used concepts from fractal mathematics.

In Euclidean geometry a straight line with length L can be measured with a measuring unit ϵ ($\epsilon \leq L$):

$$L(\epsilon) = N\epsilon^1 = \text{constant} \qquad [2.4.11]$$

with : N - number of measuring units to cover straight line

This holds also true for two or three dimensions, when the exponent of ϵ

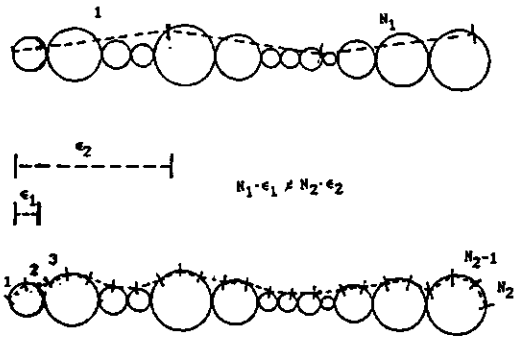

fig. 2.4.1. Dependence of the length of an irregular line on the length of the measuring unit (after: Tyler and Wheatcraft, 1989)

is changed to 2.0 or 3.0 respectively.
If the line is irregular, the measured length becomes dependent of the size of the measuring unit (see figure 2.4.1). In that case the following relationship holds:

$$F = N\epsilon^D = \text{constant} \qquad [2.4.12]$$

with : F = measure of line length, independent of ϵ
D = dimension that yields a constant F

Combining equations 2.4.11 and 2.4.12 yields:

$$L(\epsilon) = F\epsilon^{1-D} \ , \qquad [2.4.13]$$

which is a transformation relationship between topological dimension of one and the fractal dimension of D for a fractal line.

The irregular line we are dealing with in the model of Arya and Paris is the pore wall. Whereas they assumed a straight capillary tube of which the length was expressed in equivalent particle radii (eq. 2.4.8), Tyler and Wheatcraft consider a pore to be a fractal object, of which the true length is measured as:

$$h_i^* = F \cdot (2R_i)^{1-D} \qquad [2.4.14]$$

with : h_i^* = true length of the pore channel

F can be evaluated from equation 2.4.12, setting $2R_i$ equal to the straight line length h_i of h_i^*, so that N=1 and:

$$F = h_i^D \qquad [2.4.15]$$

The true fractal pore length of the i-th scale of measurement in terms of particle size and straight line length is then given by:

$$h_i^* = h_i^D(2R_i)^{1-D} \qquad [2.4.16]$$

But h_i is equal to $2R_iN_i$ so,

$$h_i^* = 2R_iN_i^D \qquad [2.4.17]$$

The exponent D is the fractal dimension describing the tortuosity of the pore channels and is equivalent to Arya and Paris' α. A low fractal dimension is an indication for a fairly straight channel, while a D of 1.5 yields a very tortuous pore channel. D > 1.5 are physically unrealistic according to Tyler and Wheatcraft.
The exponent α, invoked by Arya and Paris to account for non-spherical particles has thus a sound physical basis.

The fractal dimension of a three dimensional packing of particles can be estimated from the following relationship:

$$NR_i^D = \text{constant} \qquad [2.4.18]$$

with : N = number of particles of radius > R_i

For D = 0 the distribution is composed of particles of equal diameter. 0 < D <3.0 reflects a greater number of larger grains, whereas D > 3.0 reflects a distribution dominated by smaller particles.
D can thus be estimated from a log-log plot N versus R_i. R_i, the representative particle radius of a fraction, was taken by Tyler and Wheatcraft to be the arithmetic mean of two successive sieve sizes. N_i can be calculated, assuming spherical particles and a known particle density (2.65 $g \cdot cm^{-3}$).
In our case we need the fractal dimension of the one dimensional trace of the

pore channel. Tyler and Wheatcraft use the concept of fractal increment D_i being the difference between the fractal dimension and the traditional topological dimension, D_T. It is assumed that the fractal increment ($D - D_T$) is constant for different topological dimensions (profiles, transects). Then the fractal dimension of the pore channel (1 dimension) can be estimated from the fractal dimension of the soil matrix D (3 dimensions), as $1 + (D - D_T) = 1 + D_i$.

2.4.3 Haverkamp and Parlange

Haverkamp and Parlange (1986) presented a model relating the soil water retention curve to the cumulative particle size distribution. They claimed the model to be applicable to sandy soils without organic matter.
To relate soil water pressure to pore radius they used the equation of capillarity (eq. 2.4.10). To relate particle diameter to equivalent pore radius they used a simple linear relation, which will hold only when pores of different sizes are similar in shape:

$$d = \gamma R \qquad [2.4.19]$$

with : d = particle diameter (cm)
R = equivalent pore radius (cm)
γ = packing parameter (-)

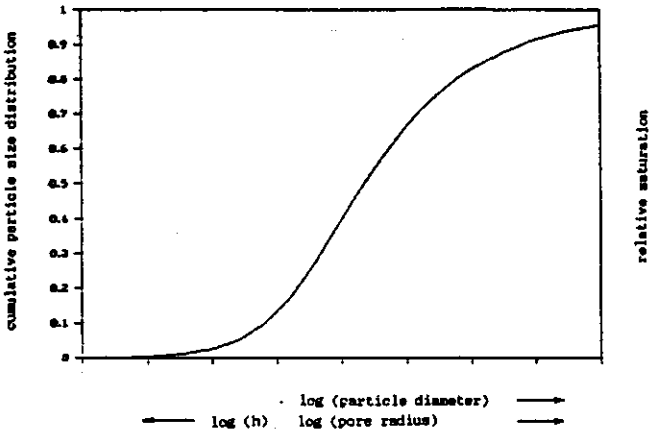

fig. 2.4.2. Shape similarity between cumulative particle size distribution and retention curve

γ is dependent on textural and structural soil properties and is a simplification of a more complex d(R) relation. The simplification, however, is justified when structural properties become independent of the degree of saturation which is the case for relatively uniform particles in sandy soils. Assuming shape similarity between the cumulative particle size distribution and the retention curve (see fig. 2.4.2) it follows from 2.4.19 that for a given R and d (= γR) the relative pore fraction and the relative solid fraction are equal:

$$S(\gamma R) = F(d) \qquad [2.4.20]$$

with : F = cumulative particle size distribution (-)
S = relative saturation = θ/θ_s (-)

When equations 2.4.10, 2.4.19 and 2.4.20 are combined with known values for θ_s and γ a water retention curve can be determined from a cumulative particle size distribution. In order to incorporate the effect of hysteresis a different value of γ should be determined for each scanning curve, because γ is the only parameter which could yield different values for R, with the same d and same packing arrangement. However, Haverkamp and Parlange selected a value for γ, consistent with one of the boundary scanning curve and predicted the other boundary curve using a hysteresis model of Parlange. For an explanation of the symbols and variables, see fig 2.4.2.

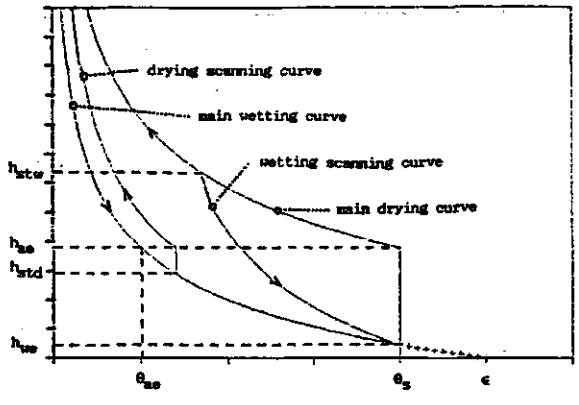

fig 2.4.2 Explanation of terms and variable occurring in model of Haverkamp and Parlange (after: Haverkamp and Parlange, 1986)

Haverkamp and Parlange used the Brooks and Corey (1964) equation to describe the main wetting curve, setting θ_r to zero, because they considered it to be a fitting parameter:

$$\left(\frac{\theta_w}{\theta_{ae}}\right) = \left(\frac{h_{ae}}{h}\right)^{\lambda} \qquad \text{for } h \geq h_{ae} \qquad [2.4.21]$$

with : θ_{ae} = water content at $h = h_{ae}$ (-)
λ = coefficient (-)

In order to circumvent the assumption that the potential at air entry and water entry (h_{ae} and h_{we}, respectively) are equal, the lower part of the wetting branch is described by the linear relationship passing through $h_{we}(\theta_{ae})$ and $h_{we}(\theta_s)$:

$$\left(\frac{\theta_w}{\theta_{ae}}\right) = \left[1 + \lambda - \lambda\frac{h}{h_{ae}}\right] \qquad \text{for } h \leq h_{ae} \qquad [2.4.22]$$

so that:

$$\theta_{ae} = \theta_s\left[1 + \lambda - \lambda\frac{h_{we}}{h_{ae}}\right]^{-1} \qquad [2.4.23]$$

A drying scanning curve, starting at a water pressure h_{std} on the wetting boundary of the loop, is given by:

$$(h - h_{std})\frac{d\theta_w}{dh} = \theta_w - \theta_d \qquad [2.4.24]$$

with : θ_w = θ for h at the wetting curve (-)
θ_d = θ for h at the drying curve (-)

Combination of equations 2.4.21 through 2.4.24 together with $h_{std}(\theta_{std}) = h_{we}(\theta_s)$, yields formulations for the main wetting and drying curves. The two specific water pressures occurring in these formulations, h_{ae} and h_{we} are of course linked, but Haverkamp and Parlange argued that the relationship is not

constant. The water entry pressure tends to zero when the pore space becomes totally saturated, when θ_s tends to the porosity ϵ:

$$\frac{h_{we}}{h_{ae}} = [\frac{1 + \lambda}{\lambda}](1 - \frac{\theta_s}{\epsilon}) \qquad [2.4.25]$$

Using this, yields the final main wetting curve:

$$\theta = \frac{\epsilon}{1 + \lambda}[\frac{h_{ae}}{h}]^{\lambda} \qquad \text{for } h > h_{ae} \qquad [2.4.26a]$$

$$\theta = \epsilon[1 - (\frac{\lambda}{1 + \lambda})\frac{h}{h_{ae}}] \qquad \text{for } h_{we} \leq h \leq h_{ae} \qquad [2.4.26b]$$

$$\theta = \theta_s \qquad \text{for } h \leq h_{ae} \qquad [2.4.26c]$$

And the main drying curve:

$$\theta = \epsilon(\frac{h_{ae}}{h})^{\lambda}[1 - \frac{h_{ae}}{h}(1 - \frac{\theta_s}{\epsilon})] \qquad \text{for } h > h_{ae} \qquad [2.4.27a]$$

$$\theta = \theta_s \qquad \text{for } h \leq h_{ae} \qquad [2.4.27b]$$

In order to use this model the parameters θ_s, λ, γ and h_{ae} (which is a function of γ) have to be estimated.
θ_s is considered as an independent input parameter.
λ has been found to be related to the pore size distribution and can be estimated from the cumulative particle size distribution F(d), assuming shape similarity between $\theta_w(h)$ and F(d). Haverkamp and Parlange use a function, similar to the Mualem-Van Genuchten equation, to describe F(d). The function contains two fitting parameters, n and d_g:

$$F = \frac{1}{[1 + (\frac{d_g}{d})^n]^m} \qquad [2.4.28]$$

with : $m = 1 - 1/n$

For high values of d, equation 2.4.28 tends to:

$$F = \left(\frac{d_g}{d}\right)^{\mu} \qquad [2.4.29]$$

with : $\mu = m/(1-m)$

Assuming shape similarity between $\theta_w(h)$ and $F(d)$, $\mu = \lambda$. This only holds for uniform-sized particle systems. Therefore μ is corrected as a function of soil structure using ρ_d:

$$\lambda = a_1 \cdot \mu \cdot \rho_d^{a2} \qquad [2.4.30]$$

with : a_1 = regression coefficient $((cm^3 \cdot g^{-1})^{-a2})$
a_2 = regression coefficient (-)

h_{ae} is related to γ and d by equation 2.4.10 and 2.4.19, where there are two values for γ, γ_{wet} and γ_{dry}, corresponding to the wetting and drying curve, respectively. Combining this with equations 2.4.10, 2.4.19, 2.4.20 and 2.4.28 yields:

$$\frac{h_{ae}}{\gamma} = \frac{2\sigma}{\rho_w g} \frac{1}{d_g}\left[\left(\frac{\theta_{ae}}{\theta_s}\right)^{-1/m} - 1\right]^{1-m} \frac{h_{ae}}{h(\theta_{ae})} \qquad [2.4.31]$$

with : $h(\theta_{ae})$ = h at θ_{ae} on the drying boundary curve
γ = γ_{dry}

Estimating θ_{ae} from the main wetting curve, and introducing it into the main drying curve yields an expression for the ratio $h_{ae}/h(\theta_{ae})$, which can be solved iteratively:

$$\frac{h_{ae}}{h(\theta_{ae})} = \left[(1+\lambda)\left[1 - \frac{h_{ae}}{h(\theta_{ae})}\left(1 - \frac{\theta_s}{\epsilon}\right)\right]\right]^{-1/\lambda} \qquad [2.4.32]$$

Finally, γ can be estimated from λ using the following regression equation:

$$\gamma = b_1 + b_2\lambda + b_3\lambda^2 \qquad [2.4.33]$$

with : b_1, b_2, b_3 = regression coefficients (-)

Combining equations 2.4.31 through 2.4.33 gives an estimate for h_{ae}.
Values for the regression coefficients used in equation 2.4.30 and 2.4.33 were obtained by Haverkamp and Parlange from 10 sandy soils, and can be found in table 2.4.1.

Table 2.4.1. Regression coefficients for the determination of λ and γ (Haverkamp and Parlange (1986))

Coefficient	Value	Coefficient	Value
a_1	0.0723	b_1	17.1736
a_2	3.8408	b_2	-4.7043
		b_3	0.1589

2.5 Spatial variability and scaling

Soil properties vary with distance, due to the spatial differences in the processes of soil formation and transformation. As a result of this variability the description of a certain soil requires a number of samples in order to obtain a representative mean. The number of samples depends on the degree of variability and the soil property under consideration.
To describe the spatial variability of soil hydraulic properties the method of scaling can be used, which is based on the concept of similar media. Similar media have internal geometries differing only by the characteristic length λ_r. This implies that such materials have identical porosities and relative particle and pore size distributions (Warrick et al., 1977).
A scaling factor α_r can be defined as:

$$\alpha_r = \lambda_r/\lambda_m \qquad [2.5.1]$$

with : λ_r - microscopic characteristic length of soil at location r
λ_m - microscopic characteristic length of a reference soil
α_r - scaling factor for soil at location r

Then, the soil water characteristic and hydraulic conductivity at any location r can be related to a reference curve, at a certain water content i (Hopmans, 1987):

$$h_{r,i} = h_{m,i}/\alpha_r \qquad [2.5.2a]$$

$$K_{r,i} = K_{m,i}\cdot\alpha^2 \qquad [2.5.2b]$$

with : $h_{r,i}$ - pressure head at water content i at location r (cm)
$h_{m,i}$ - pressure head at water content i for reference soil (cm)
$K_{r,i}$ - conductivity at water content i at location r ($cm.hr^{-1}$)
$K_{m,i}$ - conductivity at water content i for reference soil ($cm.hr^{-1}$)

Assuming the similar media concept to be valid, the soil hydraulic properties of an area could be described by a reference retention curve and conductivity curve, combined with a set of scaling factors, one for each location. Real soils at adjacent locations do not satisfy the requirements for similar media in at least one aspect, viz. they do not have identical porosities. This deviation can easily be circumvented by using relative saturation S instead of θ. There may be, however, also other deviations from the concept of similar media.
A variety of methods to obtain scaling factors from measured data does exist, of which Hopmans (1987) gave a review. In this research a modification of the method of Warrick et al. (1977) is used. Scaling factors are obtained by minimizing the sum of square deviations (eq. 2.5.3a), under the condition of equation 2.5.3b:

$$SSQ = \sum_{r,i}[h_{m,i} - \alpha_r\cdot h_{r,i}]^2 \qquad [2.5.3a]$$

$$(\alpha_1 + \alpha_2 + \alpha_3 + ... + \alpha_R)/R = 1 \qquad [2.5.3b]$$

with : R - number of locations

Whereas Warrick et al. (1977) used a power function to describe $h_m(S)$ and $K_m(S)$, in this research the Van Genuchten functions will be applied (eq. 2.1.2 and 2.1.3). To scale retention data, use will be made of the PASCAL program HSCALE, written by Droogers.

2.6 Materials

All soil sample used in this research were taken from the 'Hupselse Beek' catchment, near Eibergen in the east of the Netherlands. Two sets of data were used, both consisting of sandy soils, although in the first data set some samples contained some peat.

Table 2.6.1. Data and used methods in set 1

Quantity	Method of determination
Textural analysis	fractions < 0.053 mm : sedimentation fractions > 0.053 mm : sieving
Organic matter	glow method
Bulk density	drying and weighing
Saturated water content	saturation, drying and weighing
Saturated conductivity	flux measurement at two pressure differences : ±1.5 cm and ±3 cm
Outflow data	Tempe pressure cell; with pressure increment of 1000 cm
Infiltration data	field measurement with infiltration rings

The first set was obtained in 1988 and consists of 72 undisturbed samples in cylinders with a diameter of 5 cm and a height of 5.1 cm. These were taken at a plot of 1 ha. A square 6x6-grid was used with a gridpoint spacing of 20 meters, taking samples at two depths (topsoil ± 10-15 cm, subsoil ± 45-50 cm). The samples were given a number, consisting of a letter and number for the two horizontal coordinates of the grid, and a number for the depth (top = 1, sub = 2), e.g. D3-4.
In table 2.6.1 a review is given of the available data of these samples, together with the methods used to obtain them. The data, excluding outflow and infiltration data, can be found in Appendix 1. One remark has to be made regarding the outflow data. During later experiments using the same equipment, it appeared that water evaporated through the tube leading from the bottom of the ceramic plate to the burette (see fig. 2.1.1). This leakage was of the order of 0.1 to 0.2 $ml \cdot day^{-1}$. More important was the leakage past the rubber O-rings. No quantitative data are available on this error, but the amount of leakage can be at least one order of magnitude larger than the leakage through the tube.

The second set of data has been published before by Hopmans and Stricker (1987)

as sampling scheme 2. These data were obtained from a field adjacent to the field of the first data set and is assumed to be representative for the latter. This set will be used as validation data.
The set consists of 28 samples from 7 locations at two depths, 2 samples at each point. Of these samples retention data were obtained by means of a sand-box, up to pressure heads of ± 500 cm. The retention data have been summarized in 28 sets of Van Genuchten data, setting θ_r to zero. Also conductivity data were collected, using the hot air method and the crust method (also up to ± 500 cm). Conductivity data, together with all retention data of each point (2 samples), were also fitted to the Van Genuchten model, setting θ_r to zero and l to 0.5, which yielded 14 sets of parameters, including K_s. These data can be found in Appendix 2.

2.7 Methods

The first part of this research will comprise the application of the pedo-transfer functions, described in sections 2.3 and 2.4, to the data of the first data set. To simplify data handling and storage the resulting curves will be summarized with a set of Van Genuchten parameters. Curve fitting will be done using the FORTRAN program RETC. In the curve fitting procedure θ_s will be held constant at its measured value, because none of the pedo-transfer functions predicts water contents sufficiently near saturation.
In order to make a statement on the quality of the thus generated curves, they will be compared to the retention data of data set 2, because no retention data are available of data set 1. For this comparison the curves will be fitted to the Van Genuchten equation with θ_r set to zero (as in data set 2). (in the remainder of this research the curves will be described by Van Genuchten parameters with θ_r as a fitting parameter). Averages will be taken of the curves of data set 1 and 2, for top and subsoil samples separately. A root mean square (RMS) criterion, between the estimated curves of data set 1 and the measured curves of set 2, will be used to compare the quality of the different pedo-transfer functions. To circumvent the effect of unequal porosities, S will be used instead of θ.
Besides, scaling will be applied, in order to study the description of spatial variability by the pedo transfer functions. Standard deviation, minimum and maximum values of the scaling factors of estimated and measured curves will be

compared. Also the correlation between scaling factors of the different pedo-transfer functions will be calculated to figure out to what extent these functions describe spatial variability in the same way. Because in the scaling procedure deviating soils can have a profound effect, the peaty soils in data set 1 will be excluded. As a selection criterion will be used an organic matter content of more than two times standard deviation above average.

The second part of this research is an attempt to improve the results of the one-step outflow optimization (see section 2.1), by adding retention data. These retention data will be derived from the pedo-transfer function, chosen in the first part.
Addition of retention data will take place in two ways. Firstly by including a point of the retention curve in the optimization. Secondly by fixing the retention curve, only optimizing the conductivity curve. The latter procedure will be repeated with different restraints on the optimized parameters. For the first procedure, the water content at 1000 cm will be used, because this should have the same effect as including $Q(t_\infty)$ in the optimization as advocated by Kool et al. (1985a).
The outcomes will be judged on the resulting average curve and the uniqueness of the solutions. Average conductivity curves will be obtained by logarithmic averaging over all samples, top and sub soil samples separately. Uniqueness will be tested by repeating the optimization procedure with three different sets of initial parameter values.

3. RESULTS

In this chapter firstly, in sections 3.1 and 3.2, the results on the pedo-transfer functions, described in sections 2.3 and 2.4, will be dealt with. In section 3.1 the implementation of the methods and computed van Genuchten parameters will be presented. In section 3.2 the results will be compared with the validation data. In section 3.3 the outcomes of the combined use of estimated retention data and outflow data in one-step outflow optimization will be reviewed.

3.1 Pedo-transfer functions

In this section the use and results of the pedo-transfer functions, described in sections 2.3 and 2.4 will be dealt with. But firstly a review of data set 1 will be given. Figure 3.1.1a and 3.1.1b show the average particle size distributions of 36 samples of topsoil and subsoil samples respectively. Most striking feature of these figures is the limited scatter around the mean curve. In table 3.1.1 the other measured quantities are reviewed. Note the high organic matter content.

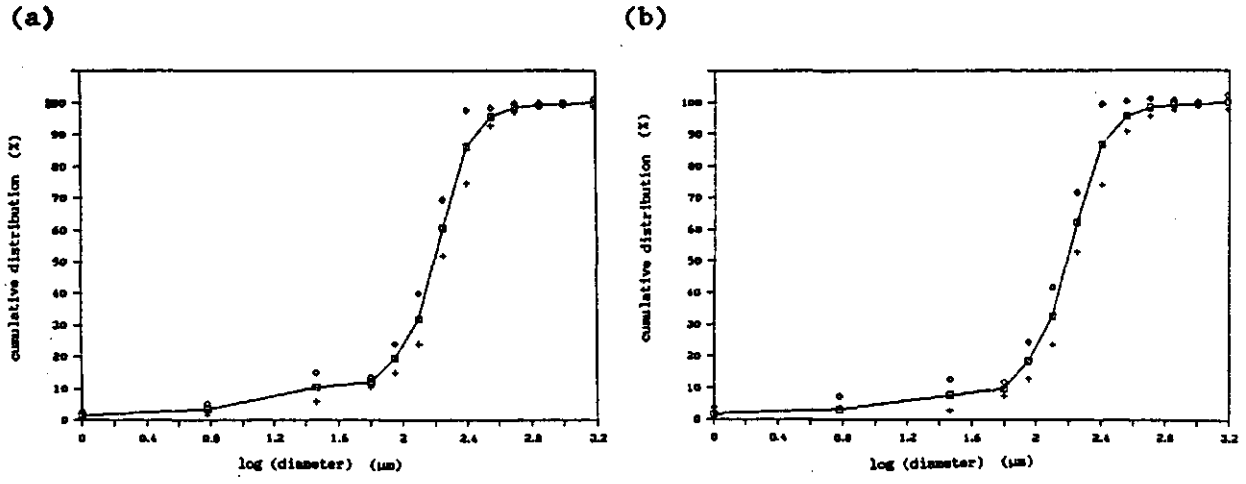

fig. 3.1.1. Average cumulative particle size distribution (□) with range ± standard deviation (+ and ◊); topsoil (a) and subsoil (b)

Table 3.1.1. Summary of data set 1

		top soil				sub soil			
Quantity	Unit	mean	SD	min.	max.	mean	SD	min.	max.
Org. mat.	%	3.677	1.919	0.89	10.5	2.085	2.115	0.35	11.18
θ_b	$g \cdot cm^{-1}$	1.442	0.120	1.02	1.59	1.514	0.146	1.1	1.77
θ_s	-	0.407	0.052	0.306	0.562	0.384	0.053	0.293	0.518
K_s	$cm \cdot hr^{-1}$	11.98	21.45	2.229	122.3	10.98	11.14	0.188	46.71
$\log(K_s)$	$cm \cdot hr^{-1}$	6.88	2.43	2.229	122.3	6.62	3.05	0.188	46.71

3.1.1 Gupta and Larson

The model of Gupta and Larson was rather easily implementable. The 13 available particle size fractions had to be reduced to percentage sand, silt and clay.

Table 3.1.1. Conversion from 13 particle-size fractions to percentage sand, silt and clay

Name	Particle -sizes	Computed as:
	μm	%
Clay (CL)	< 2	(< 2 μm)
Silt (SI)	2-50	(< 16 μm) - (< 2 μm) + 0.9513·(16-53 μm)
Sand (SA)	50-2000	0.0487·(16-53 μm) + (53-75 μm) + (75-106 μm) + + (106-150 μm) + (150-212 μm) + (212-300 μm) + + (300-425 μm) + (425-600 μm) + (600-850 μm) + + (850-1190 μm) + (>1190 μm)

This conversion can be found in table 3.1.2. Interpolation between 16 and 53 μm was done logarithmically.

The matric potentials at which water contents are computed had to be converted from bar to cm. This was done by multiplying with 1019.1 $cm \cdot bar^{-1}$. Next the Van Genuchten model was fitted to the calculated data points with θ_s held at its measured value. The result can be found in table 3.1.3.

As can be seen from the correlation coefficient R^2, the Van Genuchten model was quite well able to describe the calculated retention points. The value of all parameters are reasonable for a sandy soil. They are of the same order as those

Table 3.1.3. Van Genuchten parameters for curves generated with method of Gupta and Larson (1979)

Parameter	Unit	top soil				sub soil			
		mean	SD	min.	max.	mean	SD	min.	max.
θ_r	-	0.0573	0.0050	0.047	0.068	0.0558	0.0099	0.042	0.0858
α	cm^{-1}	0.0419	0.0139	0.0175	0.0972	0.0520	0.0190	0.0173	0.1004
n	-	1.5672	0.0379	1.4931	1.6594	1.6338	0.1362	1.4953	2.1393
R^2	-	0.9949	0.0021	0.9898	0.9983	0.9916	0.0041	0.9803	0.9978

occurring in the validation data set (appendix 2), except for α, which is about a factor 2 higher.

3.1.2 Rawls and Brakensiek

Concerning the ease of implementation and the conversion of pressure heads and particle size fractions, this model identical to that of Gupta and Larson. However, when we look at the resulting Van Genuchten parameters (see table 3.1.4) the differences appear.
Firstly, as can be seen from R^2, the retention points could not accurately be described by the Van Genuchten model. Secondly, the fitted curves sometimes have unrealistic parameter values, especially for n.

Table 3.1.4. Van Genuchten parameters for curves generated with method of Rawls and Brakensiek (1982)

Parameter	Unit	top soil				sub soil			
		mean	SD	min.	max.	mean	SD	min.	max.
θ_r	-	0.0872	0.0228	0	0.1043	0.0803	0.0196	0	0.1229
α	cm^{-1}	0.0170	0.0042	0.0112	0.0317	0.0150	0.0025	0.0104	0.0254
n	-	2.4637	1.6494	1.1770	7.4892	5.7100	4.8745	1.1864	28.119
R^2	-	0.7894	0.0470	0.7246	0.9176	0.8530	0.0682	0.6486	0.9345

3.1.3 Saxton, Rawls, Romberger and Papendick

To begin with, it should be noted that, strictly speaking, the model of Saxton et al. (1986) is not applicable to the data set under consideration. This is a consequence of the fact that Saxton et al. removed all data points with textures with > 60% clay, < 5% clay and < 5% sand from their artificial data set (see section 2.3.3). Besides, they fixed organic matter content at 0.66 %. Therefore, the curves calculated from the present data set are beyond the range of validity of the model.

The implementation of the model was not too complicated, except for the fact that some coefficients had to be adjusted, because Saxton et al. used kPa as unit of pressure head instead of cm. After the calculation of the parameters describing the various stretches of the retention curve, 16 points of the curve were calculated, namely at h=0, h_{ae}, halfway h_{ae} and 10 kPa, 10 kPa and 12 points up to h=16 kPa (logarithmically spaced).

Results of the curve fitting with the Van Genuchten model can be found in table 3.1.5. The Van Genuchten model is able to describe the points reasonably. The angular shape (round h_{ae}) of the curves generated by the model of Saxton et al. might have caused some problems. The values of α and θ_r seem acceptable, but n shows some extreme results. However, these high n values are invariably correlated to lower α values, so that the combined effect on the curves might not be as dramatic as expected (see section 2.1).

Table 3.1.5. Van Genuchten parameters for curves generated with method of Saxton et al. (1986)

Para-meter	Unit	top soil				sub soil			
		mean	SD	min.	max.	mean	SD	min.	max.
θ_r	-	0.0625	0.0140	0.0319	0.0989	0.0550	0.0146	0.030	0.0897
α	cm^{-1}	0.0184	0.0053	0.0105	0.033	0.0215	0.0070	0.0112	0.0354
n	-	3.5361	4.1792	1.5135	23.996	2.7623	1.9112	1.4813	11.582
R^2	-	0.9753	0.0109	0.9536	0.9957	0.9803	0.0113	0.9561	0.9965

3.1.4 Cosby, Hornberger, Clapp and Ginn

Implementation of the model of Cosby et al. consisted of two steps. Firstly the parameters of equation 2.3.7 were calculated. No correlation ($R^2 \approx 0.01$) appeared to exist between the θ_s and K_s as calculated with the regression equation and the values which are reported data set 1 (appendix 1).
Next, for each sample 12 points of the retention curve were calculated, ranging from h_s to h=16000 cm. To make optimum use of the available data, measured values were used for θ_s, instead of estimated data.

Table 3.1.6 Van Genuchten parameters for curves generated with method of Cosby et al. (1984)

Parameter	Unit	top soil				sub soil			
		mean	SD	min.	max.	mean	SD	min.	max.
θ_r	-	0.0284	0.0044	0.02	0.041	0.0266	0.0047	0.0191	0.0393
α	cm^{-1}	0.0848	0.0010	0.0817	0.0863	0.0859	0.0015	0.0818	0.0876
n	-	1.5329	0.0172	1.4955	1.5634	1.5325	0.0285	1.4303	1.5636
R^2	-	0.9932	0.0002	0.9928	0.9935	0.9433	0.0002	0.9928	0.9936

The resulting Van Genuchten parameters can be found in table 3.1.6. The most striking fact is the lack of variability in, especially, α and n. This is attributable to two reasons. Firstly, as a result of the smoothing effect of regression equations (seeking 'average' relationships), the real variability of retention curves might be lost. This argument, however, is equally applicable to the pedo-transfer functions discussed before. A second argument is that the model of Cosby et al. makes use of only one type of curve (whereas Saxton et al, use 3 sections). This single curve is similar in shape for all textures, causing the Van Genuchten parameters not to vary much. Further, the high values of α should be noted.

3.1.5 Arya and Paris

The application of the model of Arya and Paris resulted in 12 points of the retention curve for each sample. The results of the Van Genuchten fitting procedure can be found in table 3.1.7.

Table 3.1.7. Van Genuchten parameters for curves generated with method of Arya and Paris (1981)

Parameter	Unit	top soil				sub soil			
		mean	SD	min.	max.	mean	SD	min.	max.
θ_r	-	0.0201	0.0088	0	0.042	0.0145	0.0121	0	0.0468
α	cm^{-1}	0.0078	0.0020	0.0051	0.0157	0.0075	0.0032	0.0045	0.0201
n	-	3.1019	0.4787	2.1851	4.0911	3.2289	0.7016	1.8385	5.2453
R^2	-	0.9841	0.0477	0.7032	0.9984	0.9881	0.0112	0.9417	0.9987

The parameter values look reasonable, although α is lower and n higher than expected from the validation data set (Appendix 2). But because the effects of α and n, on the shape of the retention curve, work in the same direction (see 2.1), these deviations might counteract.
One remark has to be made, which is equally applicable to the model of Tyler and Wheatcraft (see next section). This is that approaching zero pressure head, the water content approaches porosity instead of saturated water content. When air-entrapment occurs (which is nearly always) the saturated water content will be overestimated. This deviation can be corrected for in two ways. Firstly, all water contents could be multiplied by the ratio θ_s/ϵ. Secondly, which would be better, is to keep θ constant at θ_s up to that value of h at which the original curve reaches θ_s. This solution, however, is mathematically more complicated. In this research no correction is applied.

3.1.6 Tyler and Wheatcraft

A first step was to calculate the fractal dimension D of the soil material. A review of the values can be found in table 3.1.8. The averages of D for top and subsoil are equivalent to values for α of 1.483 and 1.476, which is higher than the 1.38 used by Arya and Paris.
Next the Arya and Paris model was applied again, now using a variable α, set equal to (D-2). The Van Genuchten parameters are given in table 3.1.9. The values do not differ too much from those of the curves generated with the conventional Arya and Paris model. However, because both α and n are lower, there might be some effect on the resulting curve, keeping in mind that α and n work in the same direction.

Table 3.1.8. Fractal dimension soils in data set 1, as calculated by the method cited by Tyler and Wheatcraft (1989)

Parameter	Unit	top soil				sub soil			
		mean	SD	min.	max.	mean	SD	min.	max.
D	-	3.483	0.1502	2.918	3.705	3.476	0.182	3.154	3.929

Tyler and Wheatcraft report that fractal dimension D can even be estimated from only three particle size fractions. D, being the slope of the log-log plot of particle diameter and number of particles larger than that diameter, in fact defines a particle size-distribution. Assuming that the theory underlying the method to estimate D is valid, a particle size distribution with any number of fractions needed, could be generated when D is known. From this extended textural data again a retention curve could be estimated with the model of Tyler and Wheatcraft. To test this idea, of all samples percentages sand, silt and clay were determined, with which D was estimated. From D a new particle size distributions was derived with 12 fractions. The resulting curves were absolutely unrealistic.

Table 3.1.9. Van Genuchten parameters for curves generated with method of Tyler and Wheatcraft (1989)

Parameter	Unit	top soil				sub soil			
		mean	SD	min.	max.	mean	SD	min.	max.
θ_r	-	0.0176	0.0106	0	0.0477	0.0124	0.0122	0	0.0441
α	cm^{-1}	0.0075	0.0120	0.0011	0.0686	0.0079	0.0099	0.0004	0.0368
n	-	3.0459	0.8585	2.1671	7.3944	3.0558	0.7150	1.8842	5.3746
R^2	-	0.9909	0.0061	0.9670	0.9980	0.9874	0.0106	0.9445	0.9981

3.1.7 Haverkamp and Parlange

This model was, compared to all others, the most time consuming, both in implementation and in computation time. This was due to the fact that two iteration procedures were involved. The first to fit a curve (eq. 2.4.28) to the cumulative particle size distribution. The second was to calculate the ratio $h_{ae}/h(\theta_{ae})$ (eq. 2.4.32).

In this case the main drying curve was calculated, for two reasons. Firstly, because usually retention curves are determined at desorption. Secondly, because the curves have to be used as additional data for the one-step outflow method, also a drying phenomenon.
16 points of the curve were calculated, namely h=0, $h=h_{ae}$ and 14 points between h=100 cm and h = 16000 cm. The Van Genuchten parameters can be found in table 3.1.10. The values look quite normal. The only noticeable fact is the reasonable spread in n for the subsoil samples.
One remark has to be made regarding the applicability of this model. It was designed for the use with sandy soils without organic matter. The soils under consideration are sandy soils, but the organic matter content is rather high. The paper, promised by Haverkamp and Parlange, containing an extension of the model, taking into account the effects of organic matter has not been published yet.

Table 3.1.10. Van Genuchten parameters for curves generated with method of Haverkamp and Parlange (1986)

Para-meter	Unit	top soil				sub soil			
		mean	SD	min.	max.	mean	SD	min.	max.
θ_r	-	0.0236	0.0298	0.0056	0.1642	0.0158	0.0179	0.0028	0.102
α	cm^{-1}	0.0098	0.0011	0.0081	0.0133	0.0102	0.0019	0.0070	0.0166
n	-	2.2614	0.5237	1.1873	3.8768	2.8416	1.2069	1.2415	6.922
R^2	-	0.9898	0.0027	0.9847	0.9984	0.9899	0.0036	0.9842	0.9981

3.2 Comparison of estimated retention curves and validation data

In this part the retention curves as estimated with the respective pedo-transfer functions will be compared with the curves of the validation data (see Appendix 2). Because the validation data contained retention data up to pressure heads of only ± 500 cm, no reasonable value of θ_r could be estimated. θ_r was therefore set to zero. In order to make a valid comparison, the curves generated with the pedo-transfer functions were again fitted to the Van Genuchten model, now with θ_r set to zero.
For each pedo-transfer function at 15 values of h, θ was calculated and averaged

over topsoil and subsoil samples separately. The same was done for the validation curves. The resulting curves can be found in figures 3.2.1a and b through 3.2.7a and b. For the retention curves of the pedo-transfer functions also the range of one time the standard deviation around the mean is indicated. From these figures it can be seen that none of the pedo-transfer functions yields a good average curve. Either they are shifted to lower soil water pressures (Cosby et al. and Gupta and Larson) or they are too steep. The latter is applicable especially to the semi-empirical models, which might be caused by the close link between the shape of particle size distribution and the retention curve.

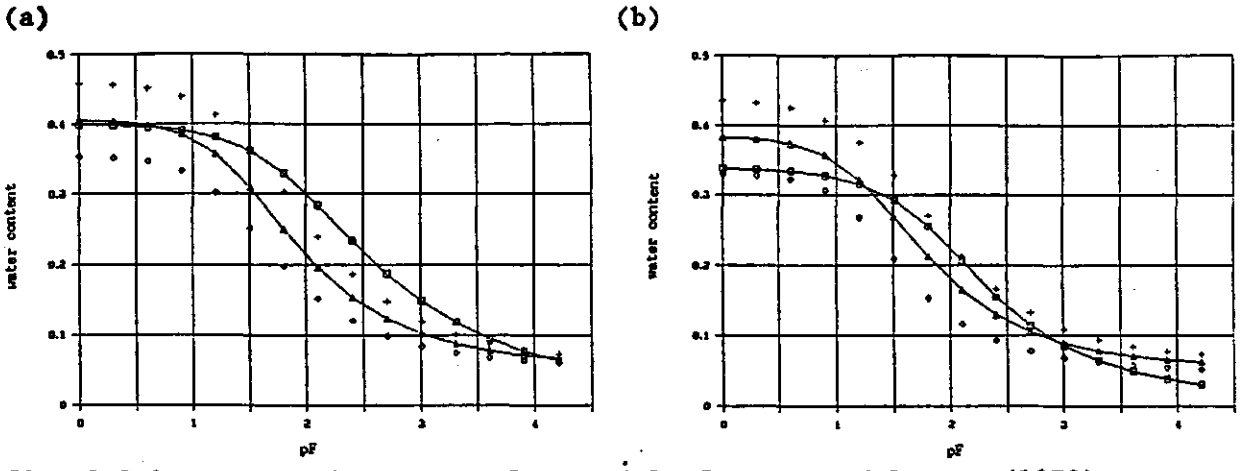

fig. 3.2.1. Retention curves from model of Gupta and Larson (1979), average retention curve (Δ) with range ± standard deviation (+ and ◊) and retention curve from validation data set (□); topsoil (a) and subsoil (b)

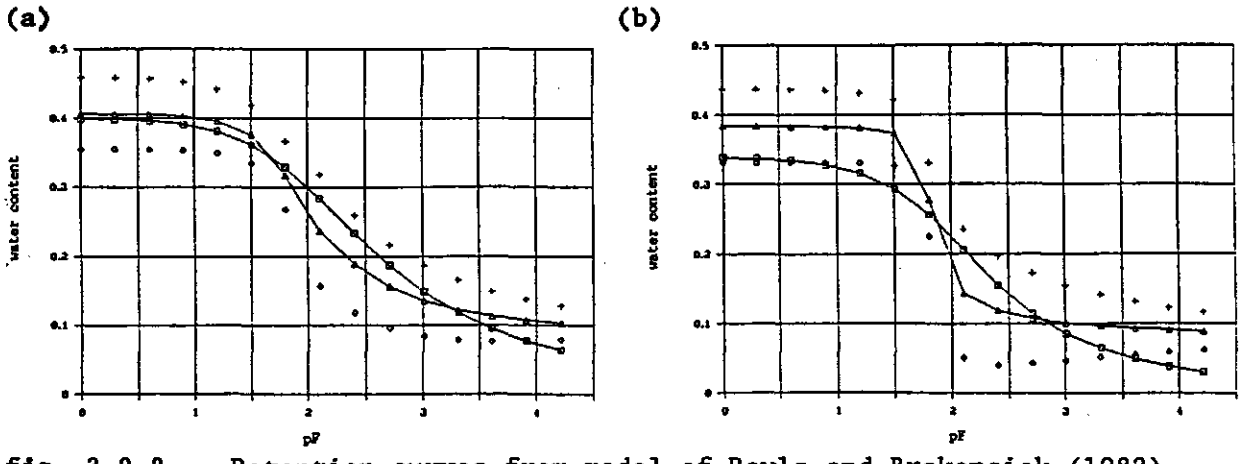

fig. 3.2.2. Retention curves from model of Rawls and Brakensiek (1982), average retention curve (Δ) with range ± standard deviation (+ and ◊) and retention curve from validation data set (□); topsoil (a) and subsoil (b)

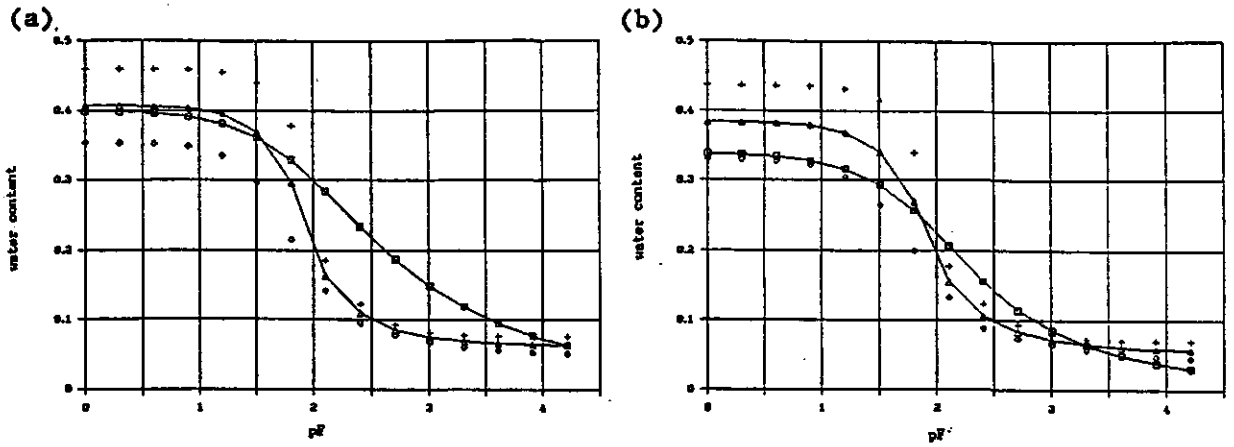

fig. 3.2.3. Retention curves from model of Saxton et al. (1986), average retention curve (Δ) with range ± standard deviation (+ and ◊) and retention curve from validation data set (□); topsoil (a) and subsoil (b)

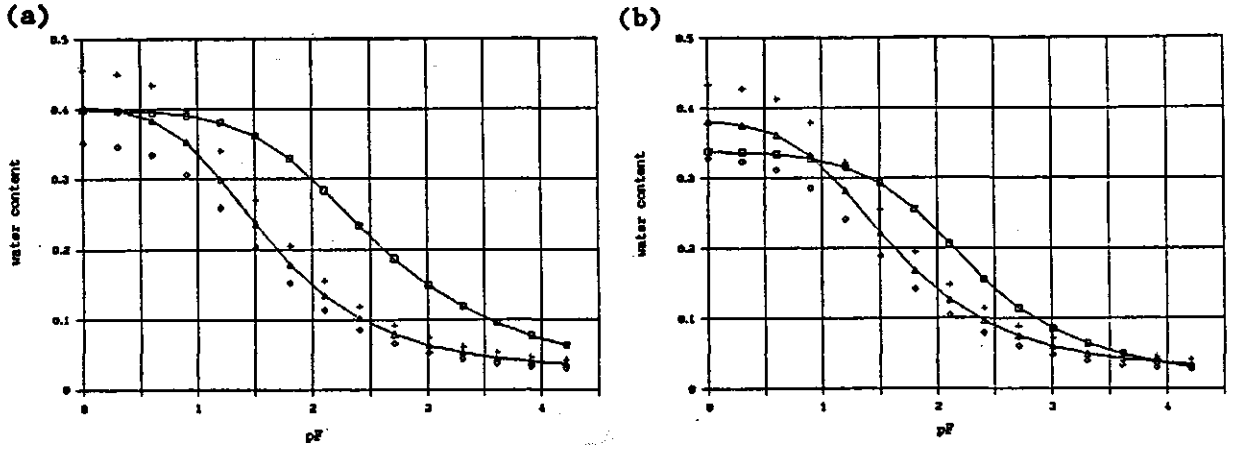

fig. 3.2.4. Retention curves from model of Cosby et al. (1984), average retention curve (Δ) with range ± standard deviation (+ and ◊) and retention curve from validation data set (□); topsoil (a) and subsoil (b)

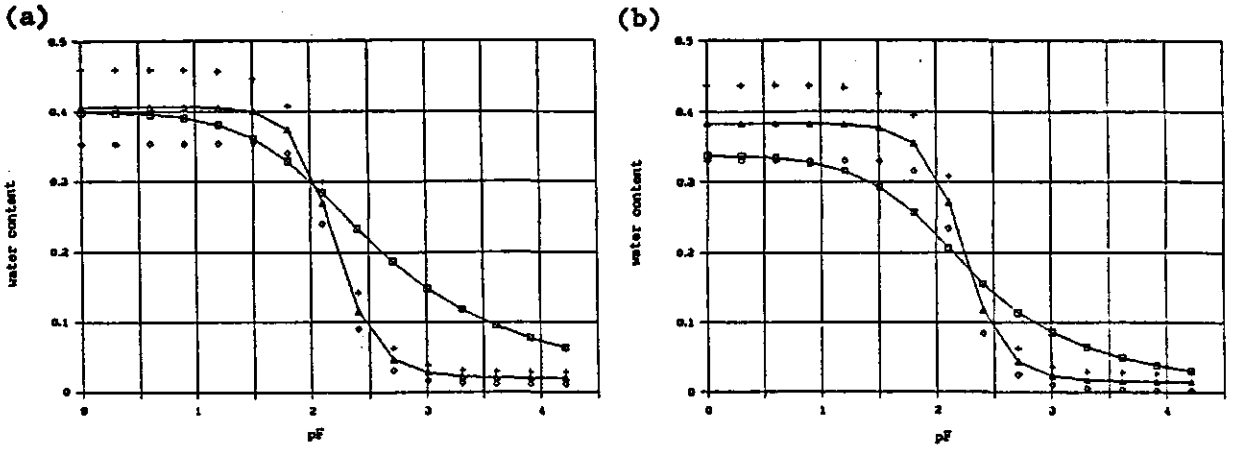

fig. 3.2.5. Retention curves from model of Arya and Paris (1981), average retention curve (Δ) with range ± standard deviation (+ and ◊) and retention curve from validation data set (□); topsoil (a) and subsoil (b)

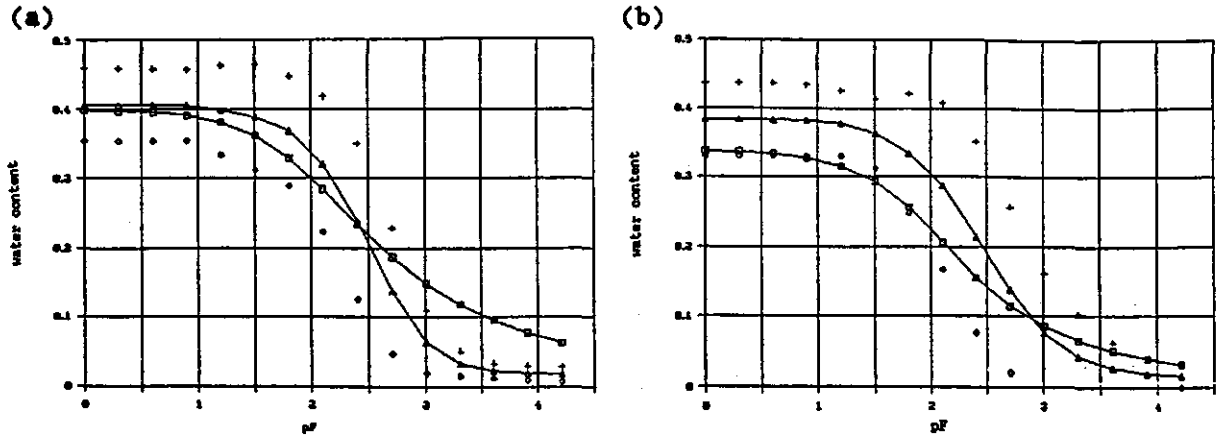

fig. 3.2.6. Retention curves from model of Tyler and Wheatcraft (1989), average retention curve (Δ) with range ± standard deviation (+ and ◊) and retention curve from validation data set (□); topsoil (a) and subsoil (b)

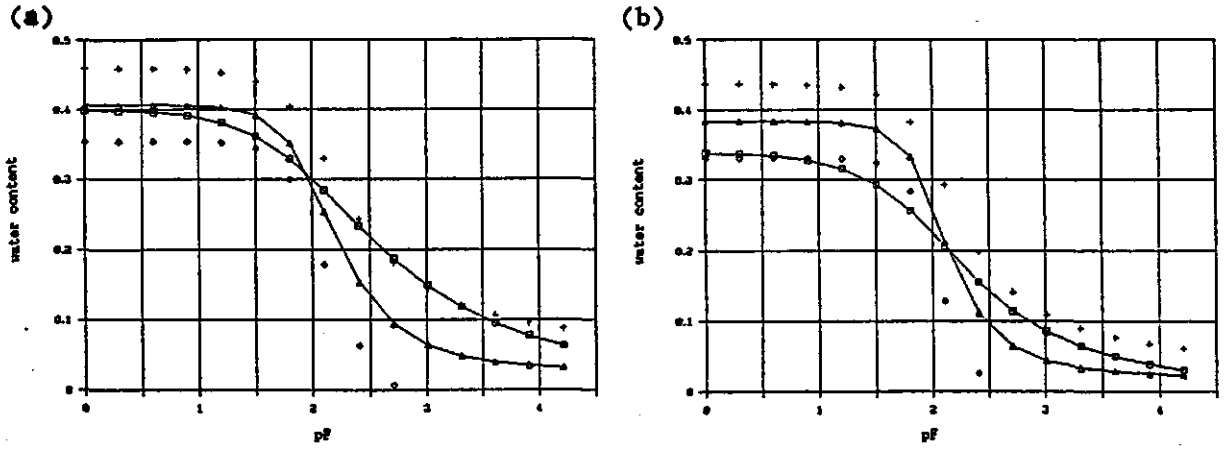

fig. 3.2.7. Retention curves from model of Haverkamp and Parlange (1986), average retention curve (Δ) with range ± standard deviation (+ and ◊) and retention curve from validation data set (□);topsoil (a) and subsoil (b)

The particle size distribution is rather steep as can be seen from figure 3.1.1.

The smoothing effect of organic matter on the retention curve is not included. Models using organic matter content as an input variable (Rawls et al. and Gupta and Larson) suffer less from this steepness syndrome.

In order to make a quantitative comparison the root mean square deviation (RMS) was calculated for each average curve. In order to circumvent the problem of comparing soils with different porosities, relative saturation S was used instead of θ. RMS is defined as:

Table 3.2.1. Root mean square deviations in S between validation curves and curves generated with pedo-transfer functions

Pedo-transfer function	Root mean square deviation	
	Top soil	Sub soil
	-	-
Gupta and Larson (1979)	0.3889	0.3337
Rawls and Brakensiek (1982)	0.4588	0.5146
Saxton et al. (1986)	0.1405	0.0856
Cosby et al. (1984)	0.6302	0.5810
Arya and Paris (1981)	0.1493	0.1008
Tyler and Wheatcraft (1989)	0.0579	0.0552
Haverkamp and Parlange (1986)	0.1106	0.0920

$$RMS = [\frac{1}{N} \sum_{i=1}^{N}((S_i)_{est} - (S_i)_{ref})^2]^{1/2} \qquad [3.2.1]$$

with : $(S_i)_{est}$ = relative saturation at h_i, at estimated curve (-)

$(S_i)_{ref}$ = relative saturation at h_i, at curve of validation data (-)

N = number of calculated points

In the calculation of RMS only retention points up to h=512 cm were used. The RMS value can be found in table 3.2.1. The most promising functions, with respect to average curves, seem to be those of Tyler and Wheatcraft, and Haverkamp and Parlange.

Also the description of spatial variability was examined by means of scaling. Because deviating soils, violating the concept of similar media, can cause large errors, soils were left out which were suspected to be peaty. As a criterion was used an organic matter content of two times standard deviation above average. Samples A1-1, D4-1, C4-2 and E5-2 were skipped. Scaling was applied separately to topsoil and subsoil curves (34 curves each).
The same was done for the validation data set, splitting it into 2 data sets (validation 1 and validation 2) because at each location two retention curves had been determined. In order to make a valid comparison possible, scaling had to be applied to that part of the retention curve where $h \leq 512$ cm. Because the scaling procedure works with a prescribed range of S, this was range was

Table 3.2.2. Distribution of scaling factors

	top soil			subsoil		
Function	$\sigma(\alpha)$	min(α)	max(α)	$\sigma(\alpha)$	min(α)	max(α)
Gupta/Larson	0.3528	0.5770	2.3738	0.4717	0.3691	2.3931
Rawls et al.	0.2335	0.5249	1.5223	0.2908	0.2912	1.2984
Saxton et al.	0.0758	0.7464	1.1218	0.1724	0.5320	1.1889
Cosby et al.	0.4860	0.8978	1.0819	0.1067	0.5878	1.0954
Arya and Paris	0.1550	0.7056	1.3238	0.2207	0.6196	1.6413
Tyler and Wheatcraft	0.5049	0.1686	2.3357	1.1664	0.0474	5.0192
Haverkamp / Parlange	0.2134	0.4782	1.5606	0.3109	0.3676	1.7269
Validation 1	0.6426	0.0124	1.9616	0.7160	0.1580	2.0570
Validation 2	0.7602	0.1142	2.4473	0.8575	0.3339	2.7436

deduced from the average retention curves of the validation data set (top soil: $S \leq 0.4$, sub soil: $S \leq 0.25$).

The resulting distribution of scaling factors can be found in table 3.2.2. The following remarks can be made. Firstly, the spread of scaling factors of Validation sets 1 and two are quite comparable. This enhances the credibility of these figures. Secondly, the limited spread for the models of Saxton et al. and Cosby et al. should be noticed. This might be result of the rigidness of the function, used to describe the retention curve. Thirdly, the distribution of the scaling factors of the model of Tyler and Wheatcraft, approximates that of the validation set most closely. Finally, it appears that the spread in scaling factors is larger for sub soil sample than for top soil samples.

In order to investigate to what extent the successive pedo-transfer functions

Table 3.2.3. Correlation between scaling factors of different pedo-transfer functions; top soil samples

	Function						
Function	Gupta Larson	Rawls et al.	Saxton et al.	Cosby et al.	Arya Paris	Tyler Wheatc.	Haverk. Parl.
Gupta/Larson	1						
Rawls et al.	0.8165	1					
Saxton et al.	0.3284	0.3228	1				
Cosby et al.	0.4338	0.4883	0.2850	1			
Arya/Paris	0.0667	0.0583	0.5332	0.0484	1		
Tyler/Wheatc.	0.0300	0.0290	-0.3676	-0.2844	0.6346	1	
Haverk./Parl.	0.5620	0.5323	0.4650	0.5600	0.1890	0.0157	1

Table 3.2.4. Correlation between scaling factors of different pedo-transfer functions; sub soil samples

	Function						
Function	Gupta Larson	Rawls et al.	Saxton et al.	Cosby et al.	Arya Paris	Tyler Wheatc.	Haverk. Parl.
Gupta/Larson	1						
Rawls et al.	0.4972	1					
Saxton et al.	0.1285	0.4749	1				
Cosby et al.	0.1880	0.3507	0.2587	1			
Arya/Paris	0.1910	-0.0523	0.3718	0.0309	1		
Tyler/Wheatc.	0.2081	-0.0588	0.2420	-0.0241	0.7800	1	
Haverk./Parl.	0.7344	0.4292	-0.0448	0.4550	0.0338	0.0466	1

describe spatial variability in the same way, correlations between sets of scaling factors were calculated. These can be found in tables 3.2.3 and 3.2.4 for top and sub soil samples respectively.

Scaling factors derived from the various methods can only be compared when the reference curves resulting from scaling are comparable. Therefore the reference curves of the empirical and semi-empirical methods are shown in fig. 3.2.8 and 3.2.9 respectively, together with the reference curve derived from the model of Tyler and Wheatcraft. This is done, because the latter model is the most promising with respect to the average curve.

Relatively high correlations are found between the models of Arya and Paris and Tyler and Wheatcraft. This is not surprising, because the latter is a modification of the first. However, where the reference curve of the model of Haverkamp and Parlange closely resembles that of the other semi-empirical models, no correlation is found between the respective scaling factors.

The reference curves of the models of Saxton et al. and Rawls and Brakensiek are also comparable (also to those of the semi-empirical models), but also in this case hardly any correlation exists between the sets of scaling factors.

The curves of Gupta and Larson and Cosby et al. are deviating, but mutually comparable and also show no correlation between their scaling factors. The outcomes are consistent between top and sub soil samples.

Based on the above analysis it is decided to continue with the model of Tyler and Wheatcraft, because of both its average behaviour and the distribution of the scaling factors. No decisive conclusions can be drawn regarding the skill of the curves of individual samples.

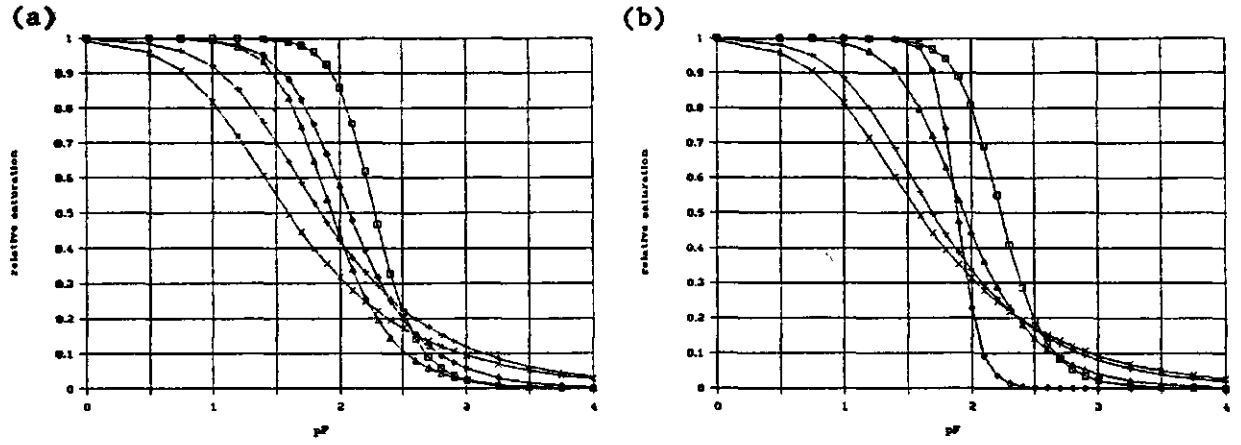

fig. 3.2.8. Comparison of reference curves obtained with scaling of retention curves from empirical models of Gupta and Larson (+), Rawls and Brakensiek (◊), Saxton et al. (Δ), Cosby et al. (×), with reference curve from model of Tyler and Wheatcraft (□); topsoil (a) and subsoil (b)

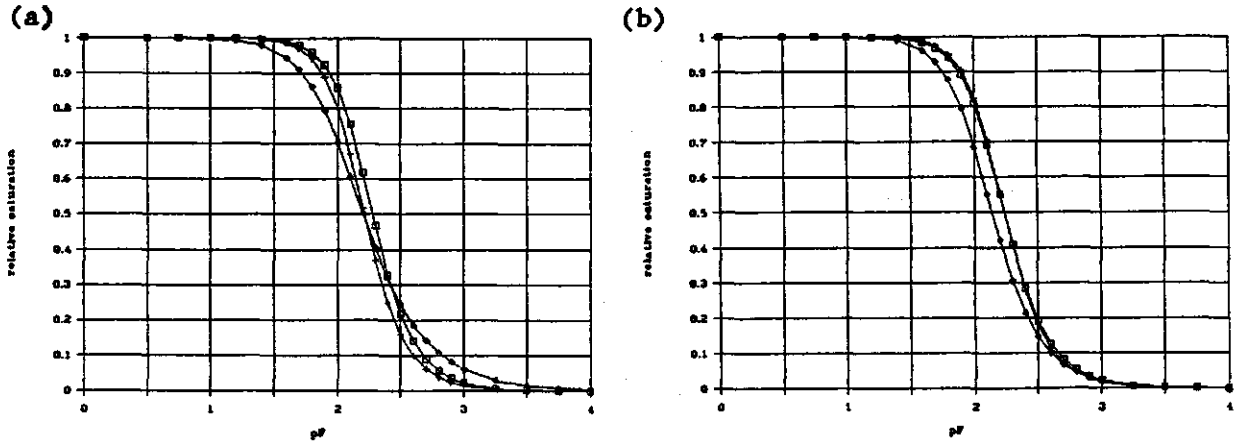

fig. 3.2.9. Comparison of reference curves obtained with scaling of retention curves from semi-empirical models of Arya and Paris (+), Tyler and Wheatcraft (□) and Haverkamp and Parlange (◊); topsoil (a) and subsoil (b)

3.3 Combination of outflow data and estimated retention curves

Available outflow data comprised cumulative outflow for a period of about six to ten hours. Times of observation were approximately logarithmically spaced in time, giving 20 to 25 readings. For some samples which drained only slowly, outflow data extend up to 15 hours. All outflows were a result of a pressure increment of 1000 cm (≈ 1 bar). The parameter optimization was executed with the program MULSTP.

Table 3.3.1. Program parameters for MULSTP

Parameter	Value	Description
NN	46	Number of nodes
LNS	42	Node at soil plate boundary
DNUL	10^{-5}	Initial time step (hr)
AIRP	1000.0	Pneumatic pressure (cm)
EPS1	1.0	Temporal weighting coefficient
EPS2	1.0	Iteration weighting coefficient
MIT	30	Maximum number of iteration
MDATA	1	Data mode (1 = transient flowdata only)

The program parameters for MULSTP, describing the optimization are given in table 3.3.1 (for a full explanation, see Van Dam et al., 1990). For all optimizations, the Mualem-Van Genuchten parameters, as derived with the model of Tyler and Wheatcraft, were used as the initial guess.
Six optimizations were performed, which are summarized in table 3.3.2. In optimization B the retention point was given a weight of 1, like every point of the cumulative outflow curve. This weighing factor might have been too low, as was indicated by Van Dam et al. (1990), who usually used a weight of 5 or more. Besides they took about five points of the retention curve into account.
A fixed retention curve (C1 to C4) implies that the optimized α and n only describe the conductivity curve, not the retention curve.

Table 3.3.2. Review of performed optimizations

Name	Input data				Constraints on parameters					
	Out-flow	Point θ(h)	Fixed θ(h)	Point K(h)	θ_s	θ_r	α	n	K_s	l
A	yes	no	no	no	fix	var	var	<var>	var	<var>
B	yes	yes	no	no	fix	var	var	<var>	var	<var>
C1	yes	no	yes	no	fix	fix	var	<var>	var	<var>
C2	yes	no	yes	no	fix	fix	var	<var>	var	var
C3	yes	no	yes	yes	fix	fix	var	<var>	var	<var>
C4	yes	no	yes	yes	fix	fix	var	<var>	var	var

Notes: Point θ(h) : water content at 1000 cm (from pedo-transfer function)
Point K(h) : measured K at saturation
<var> : 1.1 < n < 10
-0.5 < l < 1.5

Table 3.3.3. Van Genuchten parameters of average curves of data set 2 (top soil samples)

Parameter	Unit	Value
θ_s	-	0.3982
θ_r	-	0.0130
α	cm^{-1}	0.0168
n	-	1.3646
K_s	$cm \cdot hr^{-1}$	1.75
l	-	0.5

In order to gain some insight in the effect of errors in the retention data, which are added to the outflow data, a simple sensitivity analysis was employed. Using the average retention and conductivity data of the topsoil samples of data set 2 (see table 3.3.3), artificial outflow data were generated. Subsequently optimizations B and C1 were executed with errors applied to α, n and θ(1000 cm) ranging from -90 to +100, -20 to +100 and -40 to +100 % respectively. The results for optimization B can be found in figure 3.3.1. In this case the parameters α and n are valid for both retention and conductivity curve (linked via the Mualem-Van Genuchten model). Results for optimization C1 are presented in figure 3.3.2 and 3.3.3.
Looking at these figures it should be kept in mind that optimization was employed with error-free outflow data. From figure 3.3.1 it can be concluded that the

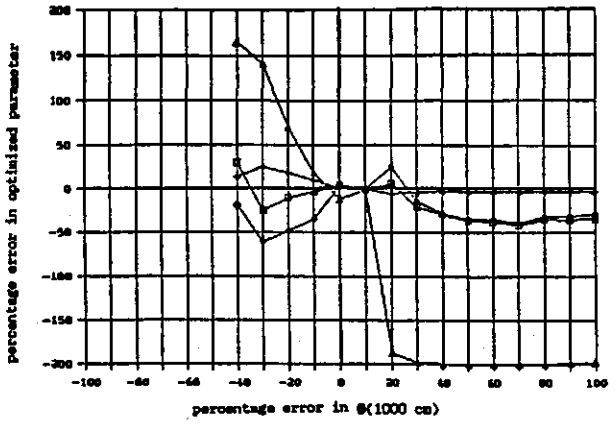

fig. 3.3.1. Sensitivity of parameter optimization to errors in additional retention data (θ(1000 cm)); optimized parameters are α (□), n (+), K_s (◊) and l (Δ)

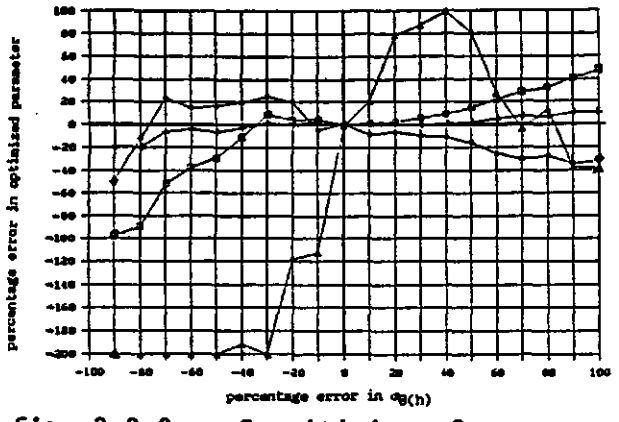

fig. 3.3.2. Sensitivity of parameter optimization to errors in α of fixed retention curve; optimized parameters are α (□), n (+), K_s (◊) and *l* (Δ)

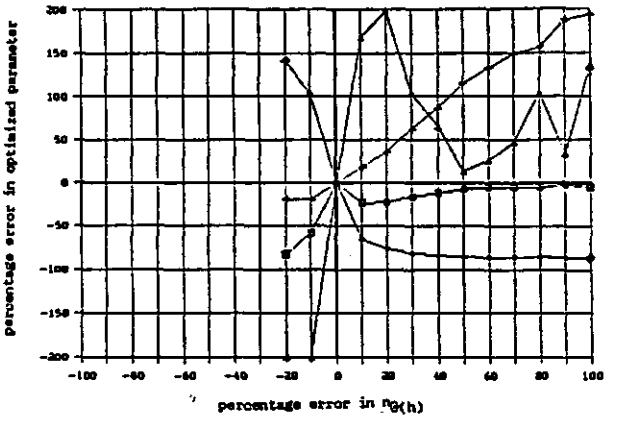

fig. 3.3.3. Sensitivity of parameter optimization to errors in n of fixed retention curve; optimized parameters are α (□), n (+), K_s (◊) and *l* (Δ)

optimization is not extremely sensitive to an error in the added retention point. When we reverse the argument, this would imply that, when outflow data are not perfect, the addition of one retention point might not be able to force the optimization into the right direction.

Figures 3.3.2 and 3.3.3 indicate that optimization C1 is more sensitive to errors in n than in α. This is however not surprising when we look at the effect of changes in parameters α, n, K_s and *l* on the shape of both retention and conductivity curve (fig. 3.3.4 through 3.3.9). The effect of a 50 % change in n is dramatic in both curves, whereas changes in α only have a minor effect. This, however, also means that retention curves, estimated with a pedo-transfer function, will have a smaller relative error for n than for α.

From this simple sensitivity analysis it might be expected that errors in the estimated retention curves give large deviations in the parameters, found in the optimization. Whether these deviations also give large errors in the resulting curves, remains to be seen. Besides, we do not know the errors in the parameters of the estimated retention curves. The average of 36 curves of the model of Tyler and Wheatcraft seemed to be a reasonable approximation of the 'real' retention curve, but the ability of the individual curves until now has not been proven.

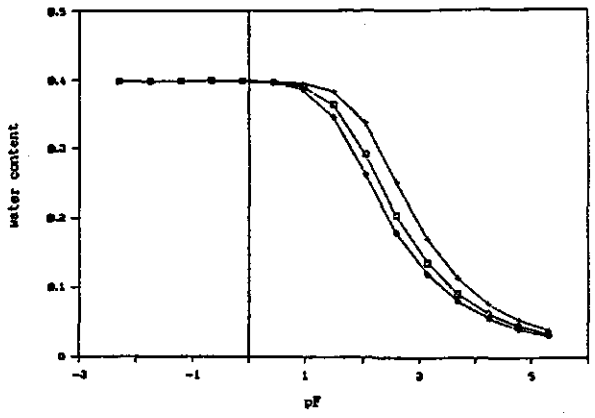

fig. 3.3.4. Effect on retention curve (□) of -50% (+) and +50% (◊) change in α

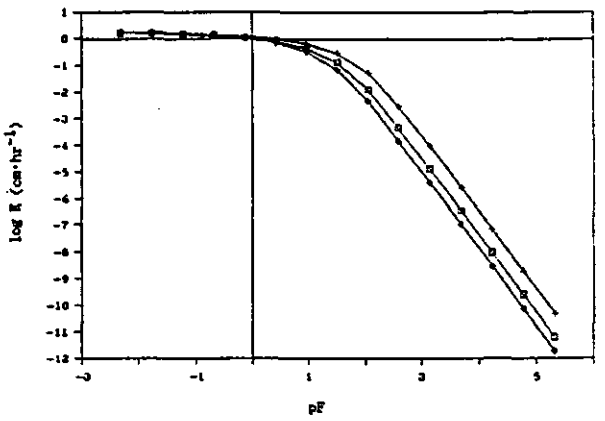

fig. 3.3.5. Effect on conductivity curve (□) of -50% (+) and +50% (◊) change in α

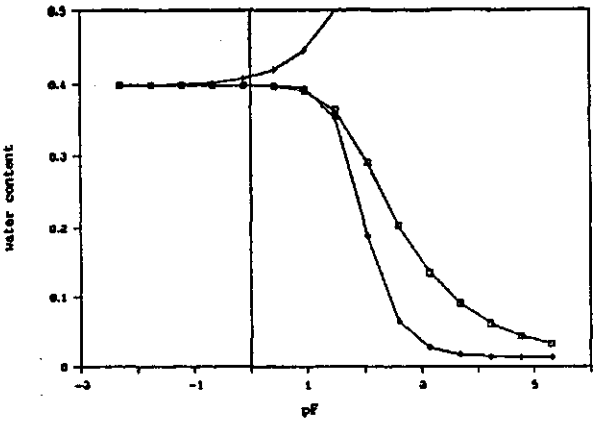

fig. 3.3.6. Effect on retention curve (□) of -50% (+) and +50% (◊) change in n

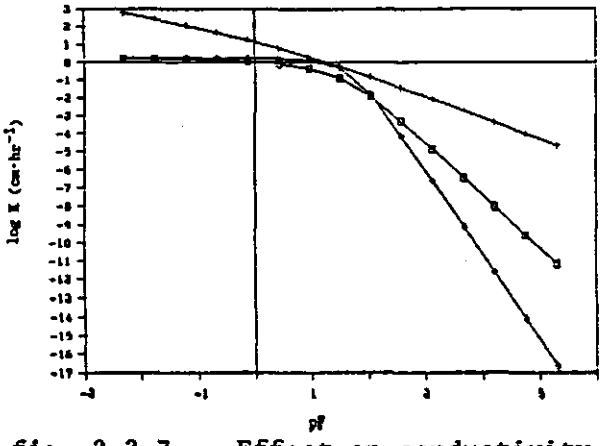

fig. 3.3.7. Effect on conductivity curve (□) of -50% (+) and +50% (◊) change in n

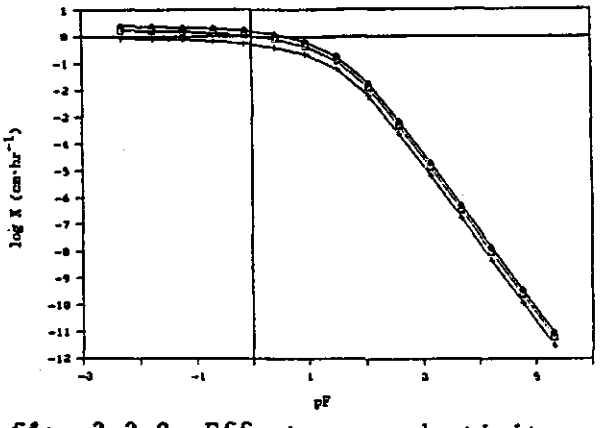

fig. 3.3.8. Effect on conductivity curve (□) of -50% (+) and +50% (◊) change in K_s

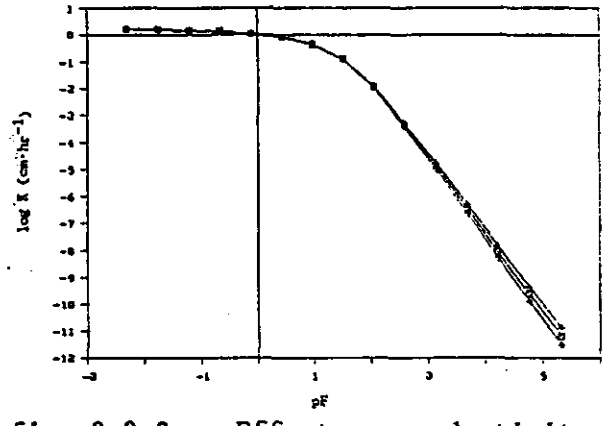

fig. 3.3.9. Effect on conductivity curve (□) of -50% (+) and +50% (◊) change in l

Regarding the simulation of the flow process, problems might arise due to non-Darcian flow. Then the equation used to describe the flow in the soil sample is not valid. In Appendix 3 it is shown that the condition of laminar flow is not violated. The condition that friction within the fluid is neglectable compared to the friction between fluid and matrix is not unambiguously fulfilled. Also at the start of the flow, say the first 15 to 60 seconds, the approximation of stationarity might not be valid. However, the effect on the optimization procedure is not clear.

Firstly optimization A was performed. A summary of the results can be found in table 3.3.4. Most striking are the high values for θ_r. The resulting amount of available water (θ_s - θ_r) is unrealistically small for some of the samples. This is partly caused by the leakages reported in section 2.6.
The high values for θ_r is also quite obvious in the figures 3.3.10a and b, showing the average retention curves of top and subsoil samples respectively. The average conductivity curves, presented in figures 3.3.11a and b, agree rather well with those of data set 2, except for the lower K_s values of the first, resulting in a downward shift. For some samples the optimization did not converge. These are mentioned in table 3.3.5. A reason for the non-convergence can be that the initial guess for the parameter values was far from the 'real' values. Addition of retention data from pedo-transfer functions obviously results in an increase in the number of non-converging optimizations. Some samples are non-converging for more than one type of optimization. This might be an indication that non-convergence is not linked to the type of optimization, but a result of a strong deviation of the added retention data from the real retention data.

Table 3.3.4. Results of optimization A

Parameter	unit	top soil (n = 35)				sub soil (n = 33)			
		mean	SD	min.	max.	mean	SD	min.	max.
α	cm^{-1}	0.018	0.014	0.001	0.050	0.022	0.017	0.003	0.059
n	-	1.430	0.232	1.1	2.248	1.507	0.242	1.187	2.168
θ_r	-	0.125	0.099	0	0.331	0.068	0.076	0	0.308
K_s	$cm \cdot hr^{-1}$	3.970	4.334	0.008	15.284	5.047	6.956	0.037	30.763
l	-	1.316	0.495	-0.5	1.5	0.898	0.856	-0.5	1.5
θ_s+θ_r	-	0.285	0.081	0.078	0.437	0.319	0.076	0.08	0.453

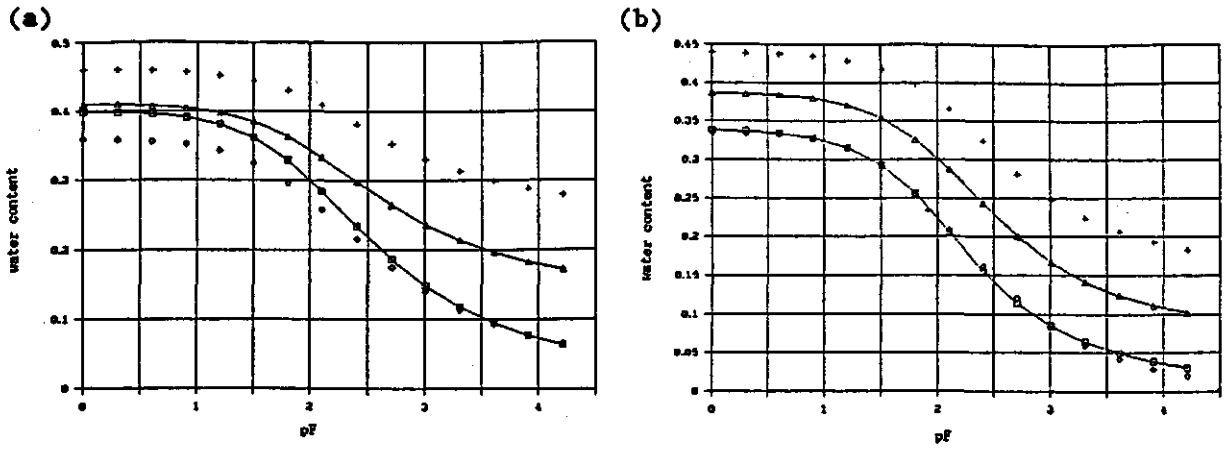

fig. 3.3.10. Retention curves from optimization A, average curve (Δ) with range of ± standard deviation (+ and ◊), together with average retention curve from validation data set (□); topsoil (a) and subsoil (b)

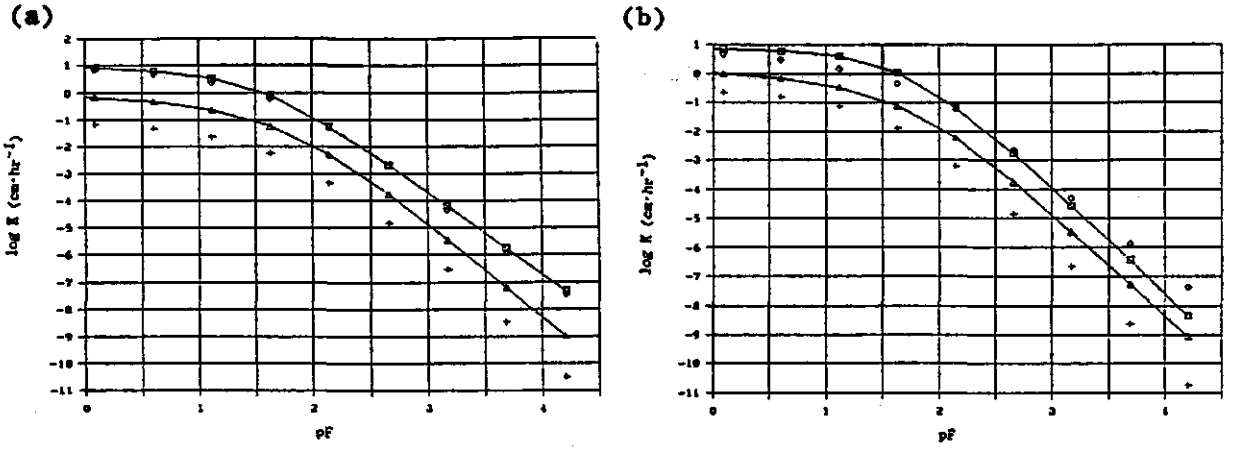

fig. 3.3.11. Conductivity curves from optimization A, average curve (Δ) with range of ± standard deviation (+ and ◊), together with average conductivity curve from validation data set (□); topsoil (a) and subsoil (b)

Optimization B, using both cumulative outflow data and one retention point (θ at 1000 cm) in the object function, presented computational problems. For a number of samples the program MULSTP entered an endless loop or encountered a division by zero, which meant that the program had to be restarted a number of times. When this optimization was repeated later, in order to test these computational problems, they did no longer occur. No explanation could be found for this.

Because of the initial computational problems, only for a limited number of topsoil samples results are available. A review of the parameters can be found in table 3.3.6. Curves are presented in figures 3.3.12 and 3.3.13.

Table 3.3.5. Samples for which optimization does not converge

Opt.	Top soil		Subsoil	
	n	sample	n	sample
A	1	E3	3	B3, D1, F3
B	10	A1, A6, C2, C3, C4, D5, D6, E3, F2, F4		
C1	5	A1, A6, B6, E3, F6	6	A6, C4, D6, F3, F4, F6
C2	11	A1, B3, B5, C2, D5, D6, E3, E4, E6, F5, F6	6	A6, C4, F2, F3, F4, F6
C3	4	A1, C2, E3, F6	4	A6, C4, F4, F6
C4	10	A1, A6, B1, B6, C2, C3, E3, E6, F4, F6	9	A6, C4, D1, E1, E2, F2, F3, F4, F6

From the results of the successful optimizations it can be concluded that optimization B obviously gives improvement, regarding the values of θ_r, which range from 0.005 to 0.10. For higher suctions, outside the experimental range, the average retention curve is too dry.

For optimization B it was also tested whether the number of non-converging samples could be reduced. This appeared to be possible by changing the initial pressure head h_0 from 0 to -5 cm. This change in h_0 can be justified by the assumption that samples, which are meant to be saturated, in reality often are incompletely saturated, giving a negative pressure head.

Table 3.3.5. Results of optimization B

Parameter	unit	top soil (n = 26)			
		mean	SD	min.	max.
α	cm^{-1}	0.009	0.011	0.001	0.043
n	-	3.982	2.001	1.695	10
θ_s	-	0.409	0.044	0.323	0.531
θ_r	-	0.051	0.044	0	0.173
K_s	$cm \cdot hr^{-1}$	1.612	7.264	0.0003	7.922
l	-	1.423	0.385	-0.5	1.5
$\theta_s-\theta_r$	-	0.35	0.062	0.226	0.479

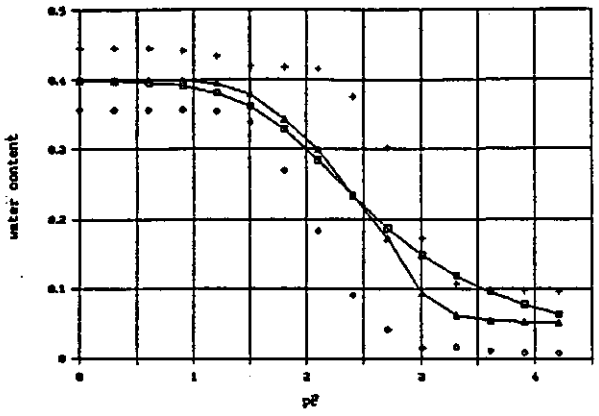

fig. 3.3.12. Retention curves from optimization B, average curve (Δ) with range of ± standard deviation (+ and ◊), together with average retention curve from validation data set (□), topsoil

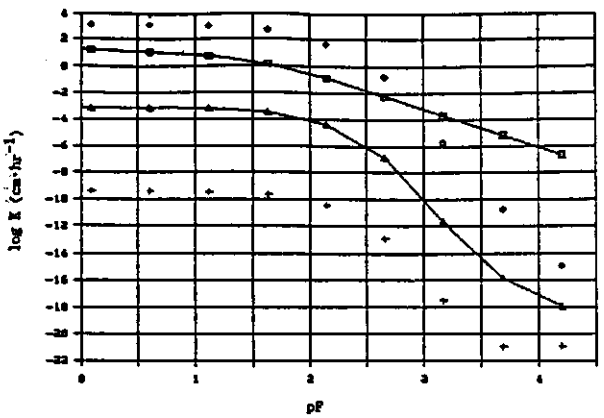

fig. 3.3.13. Conductivity curves from optimization B, average curve (Δ) with range of ± standard deviation (+ and ◊), together with average conductivity curve from validation data set (□), topsoil

Subsequently four optimizations (C1 to C4) were executed, fixing the parameters of the retention curve to those obtained from the Tyler and Wheatcraft model, optimizing for the parameters of the conductivity curve only. The results of these optimizations are presented in table 3.3.7, while the resulting average conductivity curves are shown in figures 3.3.14 through 3.3.17. Inclusion of K_s in the data of the object function (optimizations C3 and C4), results for almost all some samples in a mere fixing of K_s at its measured value. For unsaturated flow-modelling the K_s as measured at saturation is often not representative for K at lower potentials, due to structural features like cracks and root channels. It would therefore be preferable to leave K_s totally free in the optimization. As can be seen in table 3.3.6 this leads for optimization C2 to a reasonable average value for K_s (compare to table 3.1.1). In the optimizations C1 and C3 *l* quite often reached the upper and lower boundary values. This was the reason for including optimizations C2 and C4, leaving *l* completely free. The range in resulting values for *l* seems to be extremely large. However, recalling that the effect of *l* on the shape of the conductivity curve is rather small, the effect of this large range on the resulting curves might not be too dramatic. A disadvantage of leaving *l* completely free is that for more samples the optimization is not converging (table 3.3.5).

Table 3.3.6. Results of optimizations in group C

Parameter	unit	top soil mean	top soil SD	top soil min.	top soil max.	sub soil mean	sub soil SD	sub soil min.	sub soil max.
		Optimization C1 (n = 31)				Optimization C1 (n = 31)			
α	cm^{-1}	0.009	0.006	0.002	0.028	0.007	0.006	0.001	0.029
n	-	5.354	2.172	1.715	10.0	4.874	2.624	1.1	10.0
K_s	$cm \cdot hr^{-1}$	4.290	17.400	0.0	99.132	3.010	6.137	0.001	24.622
l	-	0.481	0.764	-0.5	1.5	0.449	0.830	-0.5	1.5
		Optimization C2 (n = 25)				Optimization C2 (n = 30)			
α	cm^{-1}	0.009	0.006	0.002	0.026	0.007	0.007	0.001	0.031
n	-	4.315	2.052	1.1	10.0	3.980	2.526	1.1	9.985
K_s	$cm \cdot hr^{-1}$	3.127	6.679	0.011	29.956	10.318	26.575	0.017	100.0
l	-	2.844	5.904	-0.675	28.517	6.310	12.790	-4.997	62.333
		Optimization C3 (n = 32)				Optimization C3 (n = 32)			
α	cm^{-1}	0.012	0.008	0.003	0.033	0.012	0.011	0.0004	0.055
n	-	3.749	1.619	1.502	10.0	3.081	1.512	1.1	7.347
K_s	$cm \cdot hr^{-1}$	11.795	19.488	0.0	100.0	9.394	9.724	1.033	42.657
l	-	1.055	0.757	-0.5	1.5	1.138	0.689	-0.5	1.5
		Optimization C4 (n = 26)				Optimization C4 (n = 26)			
α	cm^{-1}	0.008	0.007	0.002	0.031	0.006	0.010	0.0004	0.054
n	-	2.714	1.631	1.101	9.142	2.239	1.166	1.1	6.755
K_s	$cm \cdot hr^{-1}$	9.850	12.029	0.011	58.468	9.387	9.548	0.037	42.684
l	-	10.990	8.948	-0.56	37.806	12.036	14.248	-3.224	61.955

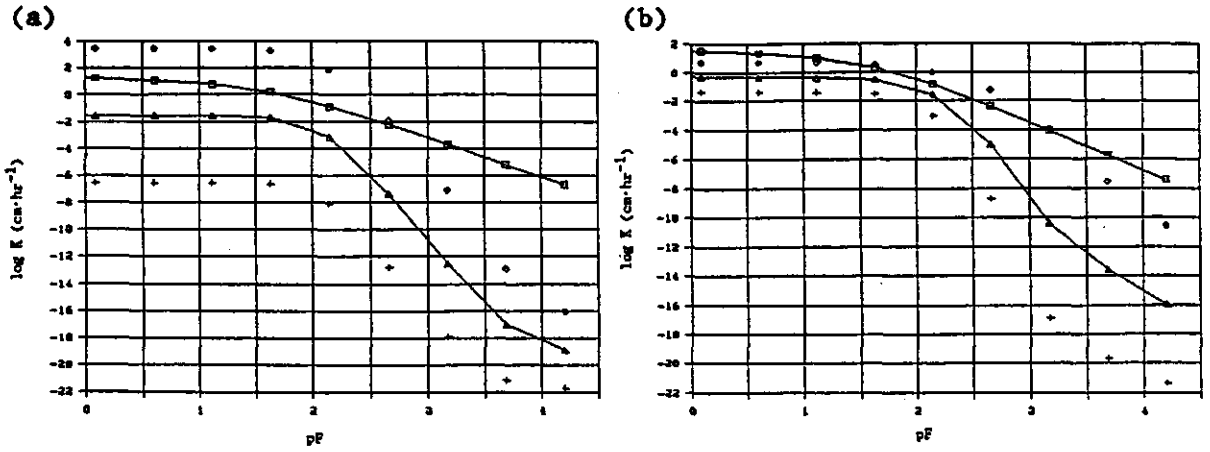

fig. 3.3.14. Conductivity curves from optimization C1, average curve (Δ) with range of ± standard deviation (+ and ◊), together with average conductivity curve from validation data set (□); topsoil (a) and subsoil (b)

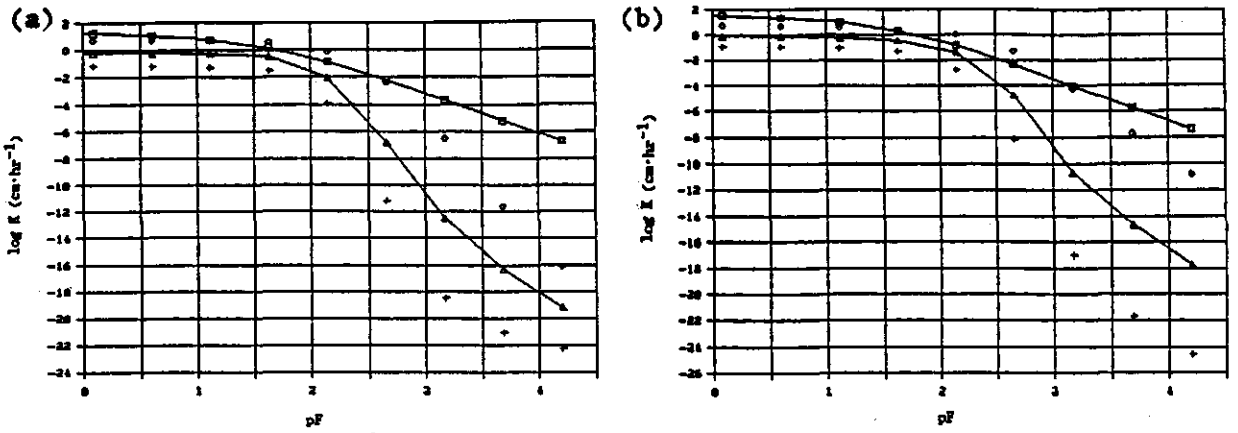

fig. 3.3.15. Conductivity curves from optimization C2, average curve (Δ) with range of ± standard deviation (+ and ◊), together with average conductivity curve from validation data set (□); topsoil (a) and subsoil (b)

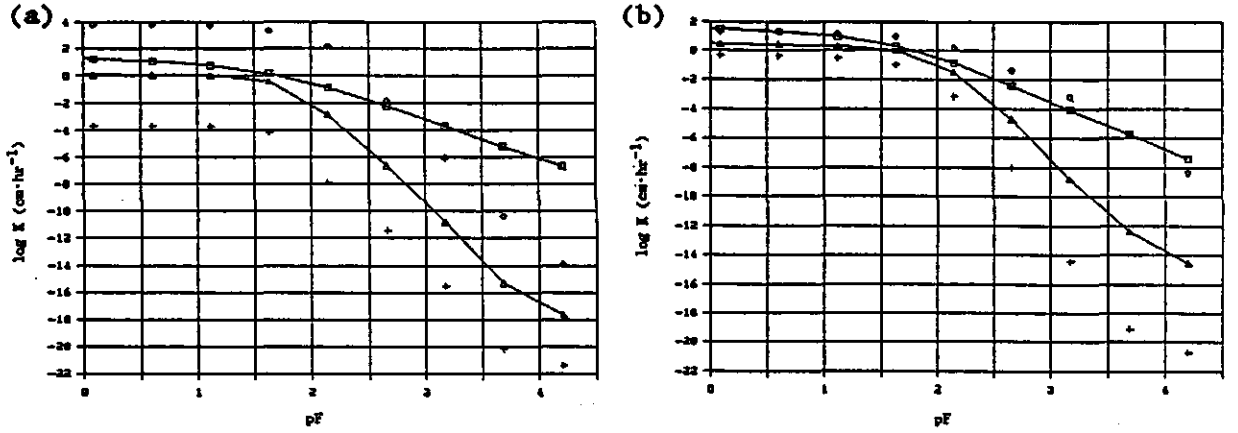

fig. 3.3.16. Conductivity curves from optimization C3, average curve (Δ) with range of ± standard deviation (+ and ◊), together with average conductivity curve from validation data set (□); topsoil (a) and subsoil (b)

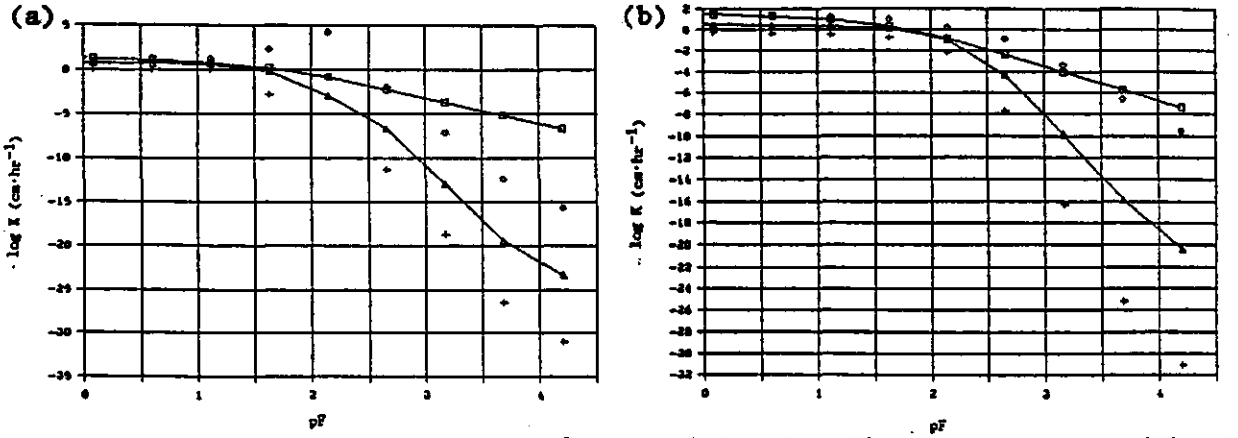

fig. 3.3.17. Conductivity curves from optimization C4, average curve (Δ) with range of ± standard deviation (+ and ◊), together with average conductivity curve from validation data set (□); topsoil (a) and subsoil (b)

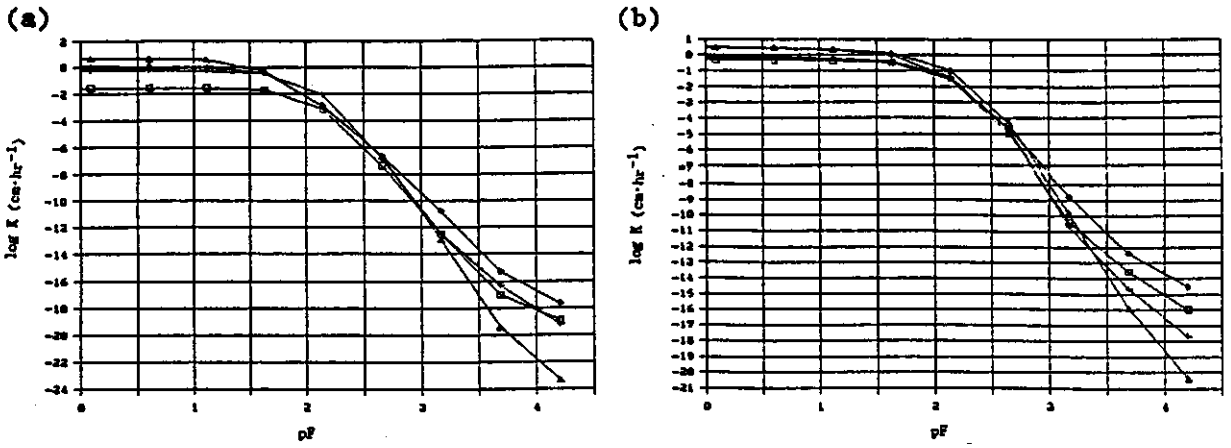

fig. 3.3.18. Comparison of average conductivity curves from optimizations C1 (□), C2 (+), C3 (◊) and C4 (Δ); topsoil (a) and subsoil (b)

A comparison is made between the average conductivity curve, resulting from the various C optimizations (fig. 3.3.18). It should be kept in mind that these curves are not always averaged over the same samples because for the various optimizations, different non-converging samples were left out. The first striking fact is that the curves of optimizations C1 through C4 hardly differ. They all deviate from the conductivity curve of the validation data set. The most obvious reason for this deviation is that if we assume that $K(\theta)$ is well predicted by the optimization, $K(h)$ is not because of the errors in $\theta(h)$, which links $K(\theta)$ to $K(h)$. It has been observed before (Stricker pers. com.,1990) that $K(\theta)$ can be rather well predicted with the one-step outflow optimization. Other reasons for the deviation between optimized $K(h)$ and those of the validation data set might be that for data set 2 unsaturated conductivity data were used up to only 512 cm ($pF \approx 2.7$) and that the parameters α, n and K_s are the result of the simultaneous fit to both retention and unsaturated conductivity data. Recently, conductivity and retention data, from the same location as data set 1, came available (Driessen et al., 1990). These data were obtained using the multi-step outflow method. The shape of the conductivity curves is about the same as that of the validation curves, based on data set 2, but the curves are shifted downward. This indicates that the α and n values are about equal but K_s is lower than in data set 2. K_s values of the recent data are more in accord with those of set 1. The average retention curves of the new data set are almost identical to those of set 2.

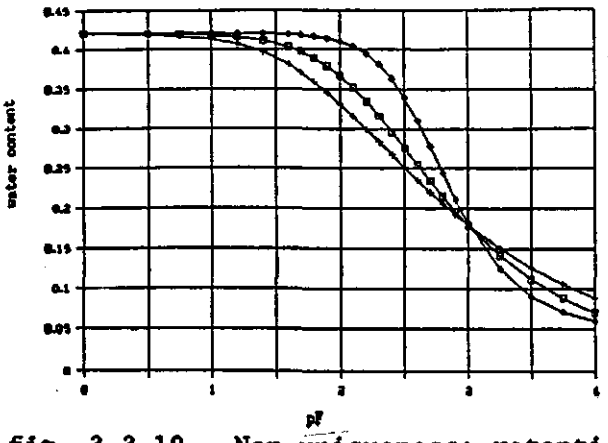

fig. 3.3.19. Non-uniqueness; retention curve of initial optimization (□) and deviating curves with RMS = 1.8 (+) and RMS = 2.6 (◊)

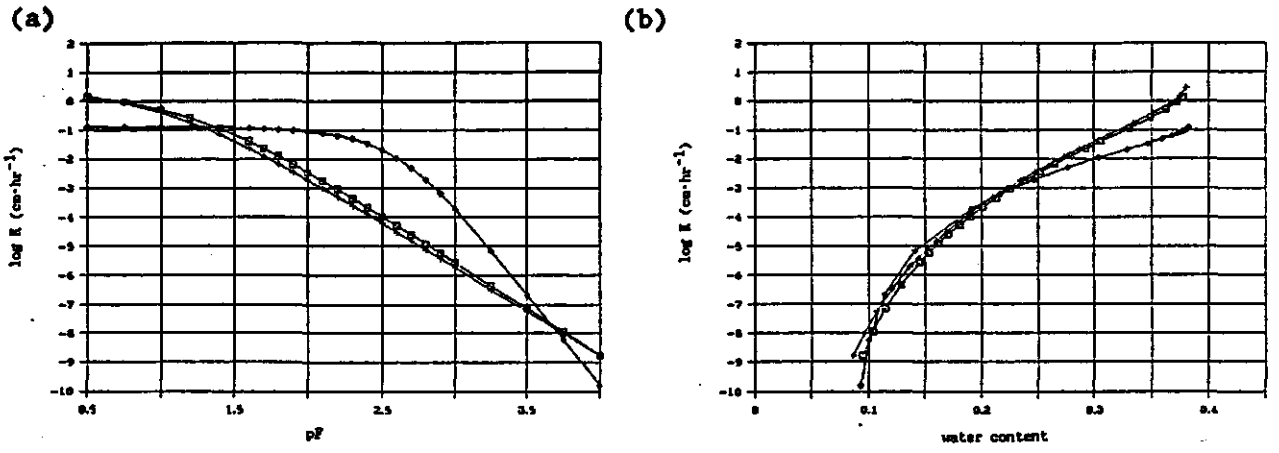

fig. 3.3.20. Non-uniqueness; conductivity curve of initial optimization (□) and deviating curves with RMS = 0.1 (+) and RMS = 0.5 (◊); deviations calculated for K(h) (a), K(θ) shown in (b)

In order to investigate the uniqueness of the optimization results, the optimizations A, B, C1 and C3 were repeated with different initial parameters (topsoil samples only). This is a standard feature of the program MULSTP. First an optimization is performed with undisturbed initial values for the parameters. In the two repetitions the initial values of α as well as n are about 50 % either larger or smaller than those of the first optimization. MULSTP calculates a Root Mean Square (RMS) (compare section 3.2) between both the retention and conductivity curve of the repetitions and the first optimization. RMS for the retention curve has the dimension of % water content. RMS for the conductivity curve indicates the order of magnitude, because $^{10}\log(K)$ is used.

In order to be able to decide whether an optimization was unique or not a threshold value of the RMS had to be selected. This selection was done by visual inspection of the effect of a certain value of RMS on the deviation

Table 3.3.8. Non-uniqueness in optimization results of topsoil samples

		for 1 repetition RMS above threshold				for 2 repetitions RMS above threshold			
		Retention		Conductivity		Retention		Conductivity	
Optimi-zation	No. of opt.	No.	%	No.	%	No.	%	No.	%
A	32	26	81.2	19	59.4	2	6.3	2	6.3
C1	29	-	-	18	62.1	-	-	3	10.3
C3	31	-	-	30	96.8	-	-	8	26.0

between curves (e.g. fig. 3.3.19). As threshold values were chosen 2.5 and 0.5 for retention and conductivity curves respectively. In figure 3.3.19 the effect of a RMS of 2.6 on the retention curve is shown. Figure 3.3.20a shows a K(h) with a RMS of 0.5.

The resulting K(θ) is shown in fig. 3.3.20b. From these two pictures it is clear that non-uniqueness in K(h) does not automatically mean non-uniqueness in K(θ).

Every sample, giving a RMS above the threshold value for at least one of the repetitions, was assumed to be non-unique for the curve under consideration. Because, for the various types of optimizations a different number of samples came to an end for both the first optimization and the two repetitions, the number of non-unique solutions is also expressed as a percentage. The results can be found in table 3.3.8. It can be concluded that the addition of a fixed retention curve yields no reduction in the non-uniqueness of the conductivity curve. Because of the computational problems with optimization B, no results are available for that optimization. From the outcomes for a small number of samples it could be concluded that also for optimization B non-uniqueness in both retention and conductivity curves was a non rare phenomenon.

If non-uniqueness is defined less restrictive, viz. if only those samples are classified 'non-unique' for which both repetitions yielded RMS values above the threshold value, the picture becomes less dramatic (see table 3.3.8). This means that we assume that, if at least one of the repetitions agrees with the first optimization (with undisturbed initial parameter values), the curve of that first optimization is the 'real' curve. The results become even better when we notice that for some samples both repetitions, having too high RMS values, yielded about the same curve. In those cases in fact the first,

undisturbed, optimization should be classified as being non-unique.
It should be noted that for most, but not all, samples the two optimizations of which the curves did agree, also had the lowest RMS values for that curve. The exceptions indicate that the result of two identical curves, from optimizations with different initial parameter values, does not guarantee that the optimization reached its global minimum.

The origins of non-uniqueness in parameter optimization results have not been investigated. The remarks made below should be seen as ideas for further research on this topic. Apart from the general remark that outflow data alone do not contain enough information to yield both a retention and a conductivity curve, there also might be a more specific sources of non-uniqueness.
In the present case some causes can be indicated. Firstly, the inaccuracies in the outflow data might have affected the presence or absence of a pronounced global minimum in the value of the object function. Secondly, the initial guess for the parameters to be optimized (derived from the model of Tyler and Wheatcraft) might have been too far from the 'real' values. Thirdly, the C-optimizations may be were forced to a wrong conductivity curve by errors in the fixed retention curve, in order to simulate an outflow close to the measured outflow. This would mean that a solution is searched at parameter values for which the object function does only have local minima. Finally, the weighing factor of 1, applied to the added retention point in optimization B might have been too low. When the extra point of the retention curve is given too less weight , it might not be able to force the optimization into the range of parameter values where the object function has its global minimum.
Apart from these causes, related to the quality of the data, there might be a more fundamental, numerical, cause. This is the shape of the response surface, which surface describes the dependence of the value of the object function on the values of the parameters to be optimized. If the response surface descends towards the 'real' parameter values over a large range of parameter values, the optimization result will not be very sensitive to the quality of the initial guess of parameter values. However when many local minima do exist near the 'real' solution, non-uniqueness might be expected.
According to Van Dam (pers. com., 1990) non-uniqueness is especially a problem for soils with extreme textures, viz. clay and sandy soils. This might be explained by different shapes of the response surface for different textures.
Also, attention should be paid to the data which the object function should

contain, in order to yield a response surface that enables the estimation of the soil hydraulic functions.

4. CONCLUSIONS

In this chapter conclusions will be drawn from the results presented in the previous chapter. Besides some suggestions for further research will be given.

The pedo-transfer functions examined in this study are all easily implementable, except for the model of Haverkamp and Parlange (1986), which requires more programming and computation time. All, but the model of Rawls and Brakensiek (1982), yield retention curves (or retention points), which can be well described by the Van Genuchten function. This is of importance, because it eases data handling and further computation.

Analysis of the resulting Van Genuchten parameters showed that there are large differences in averages and ranges of parameters. Ranges seem too small for the models of Cosby et al. (1984) This is probably caused by the rigidness of the function of the function used to describe $\theta(h)$. The models of Saxton et al. (1986) and Rawls and Brakensiek (1982) sometimes yield unrealistic values for n. The models of Arya and Paris (1981), Tyler and Wheatcraft (1989) and Haverkamp and Parlange (1986) give extreme values for α. This might be due to the assumed strong link between the shape of the retention curve and the cumulative particle-size distribution, which can be extremely steep for sandy soils.

The comparison of average retention curves of the field under consideration and the validation plot is not encouraging, regarding the skill of the pedo-transfer function. Looking at a RMS criterion, the semi-empirical models have a closer fit to the retention curve of the validation data set, than the purely empirical methods. However, from visual inspection it is quite clear that the even the semi-empirical models give a rather poor fit, especially regarding the shape of the curves. This shape reveals the true origin of these curves, viz. the cumulative particle-size distribution. Apparently the latter does not contain enough information to describe the retention curve.
In the present case the missing information might be the organic matter content, which is rather high for the data set under consideration. Influencing aggregation and the physical interaction between water and soil matrix, this high organic matter content probably is the cause of the rather smooth retention curve of the validation data set.

Regarding the description of spatial variability by pedo-transfer functions, the various models widely differ. Regarding the distribution of scaling factors, the curves of the model of Tyler and Wheatcraft most closely resemble those of the validation data set. Looking at the correlation between the scaling factors of the various pedo-transfer functions, reasonable correlations are found between the models of Arya and Paris and Tyler and Wheatcraft. Hardly any correlation is found between these two models and all others. The empirical models show hardly any correlation. These mutual inconsistencies cast some doubt on the concept of pedo-transfer functions, for one would expect at least comparable results from models which use the same input data.
The Tyler and Wheatcraft model was chosen to be the 'best' and was used to be combined with one-step outflow data.

The average retention curve, resulting from optimization on outflow data alone, has a unrealistically high residual water content, while the conductivity curve matches well with that of the validation data set when the difference in K_s is overlooked.
Both the addition of a single retention point and the addition of a fixed retention curve, both derived from the model of Tyler and Wheatcraft, yield an average conductivity curve with a rapidly decreasing conductivity, with increasing suction. When we combine this with the steep retention curve, this seems logical. The flow problem is simulated with a $K(\theta)$ relation which is related to $K(h)$ by $\theta(h)$. Thus, probably the $K(\theta)$ curve is well predicted, but due to the false $\theta(h)$, the $K(h)$ is deviating.

For the present set of outflow data, non-uniqueness of the optimization indeed is a major problem. It is clearly shown that neither the addition of a single point of the retention curve, nor a fixed retention curve, both derived from the model of Tyler and Wheatcraft, to the outflow data gives an improvement.

From the foregoing it is concluded that the pedo-transfer functions, examined in this research, can not be used to generate retention data which are accurate enough to supplement one-step outflow data.

Some topics related to the pedo-transfer functions require further research. Firstly, the inclusion of the effects of organic matter into one of the semi-empirical pedo-transfer functions should be investigated. Secondly, one of the

purely empirical pedo-transfer functions, which uses organic matter as an input variable (e.g. the model of Rawls et al. (1982)) should be tested for in the combination with outflow data. Thirdly, it remains to be seen whether pedo-transfer functions can generate accurate retention data per sample or only when averaged over a certain number of samples. This is of importance for the question whether pedo-transfer functions can ever be used for the study of spatial variability of soil hydraulic properties. Finally, pedo-transfer functions should be tested with respect to their skill in predicting some functional criteria, like capillary rise at a given depth of the water table and a given suction at top of the soil column.

Regarding the parameter optimization the problem of non-uniqueness should be investigated further. Special attention should be paid to the shape of the response surface, because that shape might be a fundamental limit to the uniqueness of solutions. The dependence of the shape of the response surface on soil texture should be looked at in order to answer the question whether non-uniqueness of the optimization results is dependent on texture. Besides, the dependence of the shape of the response surface on the kind and amount of data in the object function should be examined.

REFERENCES

Arya, L.M. and J.F. Paris, 1981. 'A physico-empirical model to predict the soil moisture characteristic from particle-size distribution and bulk density data'. **Soil Sci. Soc. Am. J.** 45 (1981), p. 1023-1030.

Arya, L.M. and J.F. Paris, 1982. 'Reply to "Comments on a physicoempirical model to predict the soil moisture characteristic from particle-size distribution and bulk density data"'. **Soil Sci. Soc. Am. J.** 46 (1982), p. 1348-1349.

Bear, J. and Y. Bachmat, 1990. '**Introduction to modelling of transport phenomena in porous media**'. Theory and applications of transport in porous media no. 4. Kluwer Academic Publishers, Dordrecht etc.

Bouma, J. and H.A.J. van Lanen, 1987. 'Extension functions and threshold values: from soil characteristics to land qualities'. In: Beek, K.J., P.A. Burrough, D.E. McCormack (eds.), 1987. '**Proceedings of the international workshop on quantified land evaluation procedures held in Washington D.C. 27 april - 2 may 1986**'. ITC Publication no. 6. ITC, Enschede, p. 106-110.

Brooks, R.H. and A.T. Corey, 1964. '**Hydraulic properties of porous media**'. Hydrology papers no. 3. Colorado State University. Fort Collins, Colorado.

Campbell, G.S., 1974. 'A simple method for determining unsaturated conductivity from moisture retention data'. **Soil Sci.** 117 (1974), p. 311-314.

Chow, V.T., D.R. Maidment and L.W. Mays, 1988. '**Applied Hydrology**'. McGraw-Hill Book Company. New York etc.

Cosby, B.J., G.M. Hornberger, R.B. Clapp and T.R. Ginn, 1984. 'A statistical exploration of the relationship of soil moisture characteristic to the physical properties of soils'. **Water Resourc. Res.** 20 (1984)6, p. 682-690.

Dam, J.C. van, J.N.M Stricker and P. Droogers, 1990. '**From One-step to Multi-step. Determination of soil hydraulic functions by outflow experiments**'. Report no. 7. Department of Hydrology, Soil Physics and Hydraulics, Agricultural University Wageningen, Wageningen.

Driessen, T, H. Huyskes and R. Overvelde, 1990. '**Hydrologisch variabiliteits onderzoek te Hupsel**' (Research on hydrologic variability in the Hupsel catchment). Velp.

Genuchten, M.Th. van, 1980. 'A closed-form equation for predicting the soil hydraulic conductivity of unsaturated soils'. **Soil Sci. Soc. Am. J.** 44 (1980), p. 892-898.

Genuchten, M.Th. van, F. Kaveh, W.B. Russell and S.R. Yates, 1989. 'Direct and indirect methods for estimating the hydraulic properties of unsaturated soils'. In: Bouma, J. and A.K. Bregt (eds.). '**Land qualities in space and time: proceedings of a symposium, Wageningen, The Netherlands, 22-26 august 1988**'. PUDOC. Wageningen.

Green, R.E., L.R. Ahuja and S.K. Chong, 1986. 'Hydraulic conductivity, diffusivity, and sorptivity of unsaturated soils: field methods'. In: 'Methods of soil analysis, part 1'. **Agronomy** 9 (1986), 2nd edition, p. 771-798.

Gupta, S.C. and W.E. Larson, 1979. 'Estimating soil water retention characteristics from particle-size distribution, organic matter percent and bulk density'. **Water Resourc. Res.** 15 (1979), p. 1633-1635.

Haverkamp, R. and J.Y. Parlange, 1982. 'Comment on a physico-empirical model to predict the soil water characteristic from particle-size distribution and bulk density data'. **Soil Sci. Soc. Am. J.** 46 (1982), p. 1348.

Haverkamp, R. and J.Y. Parlange, 1986. 'Predicting the water-retention curve from particle-size distribution: 1. Sandy soils without organic matter. **Soil Sci.** 142 (1986), p. 325-339.

Hopmans, J.W., 1987. 'A comparison of techniques to scale soil hydraulic properties'. **J. of Hydrology** 93 (1987), p. 241-256.

Hopmans, J.W. and J.N.M Stricker, 1987. '**Soil hydraulic properties in the study area Hupselse Beek as obtained from three different scales of observation: an overview**'. Publication 78. Department of Hydraulics and Catchment Hydrology, Agricultural University Wageningen. Wageningen.

Kabat, P. and M.J.P. Hack-ten Broeke, 1989. '**Input data for agrohydrological simulation models: some parameter estimation techniques**'. Report no. 9. The Winand Staring Centre. Wageningen.

Klute, A., 1986. 'Water retention: laboratory methods'. In: Klute, A. (ed.), 1986. 'Methods of soil analysis, part 1'. **Agronomy** 9 (1986), 2nd edition, p.635-662.

Klute, A. and C. Dirksen, 1986. 'Hydraulic conductivity and diffusivity:

Laboratory methods. In: Klute, A. (ed.), 1986. 'Methods of soil analysis, part 1'. **Agronomy** 9 (1986), 2nd edition, p. 687-734.

Kool, J.B., J.C. Parker and M.Th. van Genuchten, 1985a. 'Determining soil hydraulic properties from one-step outflow experiments by parameter estimation: I. Theory and numerical studies'. **Soil Sci. Soc. Am. J.** 49 (1985), p. 1348-1354.

Kool, J.B., J.C. Parker and M.Th. van Genuchten, 1985b. **'ONESTEP; A nonlinear parameter estimation program for evaluating soil hydraulic properties from one-step outflow experiments'**. Bulletin 85-3. Virginia Agricultural Experiment Station. Blacksburg.

Mualem, Y., 1976. 'A new model for predicting the hydraulic conductivity of unsaturated porous media'. **Water Resour. Res.** 12 (1976), p. 513-522.

Parker, J.C., J.B. Kool and M.Th. van Genuchten, 1985. 'Determining soil hydraulic properties from one-step outflow experiments by parameter estimation: II Experimental Studies'. **Soil Sci. Soc. Am. J.** 49 (1985), p. 1354-1359.

Rawls, W.J. and D.L. Brakensiek, 1982. 'Estimating soil water retention from soil properties'. **J. Irrig. & Drainage Div. ASCE** 108(IR2) (1982), p. 166-171.

Rawls, W.K., D.L. Brakensiek and K.E. Saxton, 1982. 'Estimation of soil water properties'. **Trans. ASAE** 25 (1982), p.1316-1320.

Vereecken, H., J. Maes, J. van Orshoven and J. Feyen, 1989. 'Deriving pedotransfer functions of soil hydraulic properties', in: Bouma, J. and A.K. Bregt (eds.). **'Land qualities in space and time: proceedings of a symposium, Wageningen, The Netherlands, 22-26 august 1988'**. PUDOC. Wageningen.

Wösten, J.H.M. and M.Th. van Genuchten, 1988. 'Using texture and other soil properties to predict the unsaturated soil hydraulic functions'. **Soil Sci. Soc. Am. J.** 52 (1988), p. 1762-1770.

Saxton, K.E., W.J. Rawls, J.S. Romberger and R.I. Papendick, 1986. 'Estimating generalized soil-water characteristics from texture'. **Soil Sci. Soc. Am. J.** 50 (1986), p. 1031-1036.

Tyler, S.W. and S.W. Wheatcraft, 1989. 'Application of fractal mathematics to soil water retention estimation'. **Soil Sci. Soc. Am. J.** 53 - (1989), p. 987-996.

Warrick, A.W., G.J. Mullen and D.R. Nielsen, 1977. 'Scaling field measured soil hydraulic properties using a similar media concept'. **Water Resour. Res.** 13 (1977), p. 355-362.

GLOSSARY

Boundary curve, see **hysteresis**

Cumulative particle size distribution, see **particle size distribution**

Cumulative pore size distribution, see **pore size distribution**

Darcy's equation describes the relationship between pressure gradient and flow velocity in a porous medium. As obtained from and experiment with a vertical, saturated, soil column by Darcy (in 1856):

$$u = -K\left(\frac{\partial h}{\partial z} + 1\right)$$

with : K = conductivity $(m \cdot s^{-1})$

It is still subject to discussion whether **Darcy's equation** can be derived from the **Navier-Stokes equation**. When this derivation is made, some assumptions have to be made, viz. stationarity, constant density, monotone pressure variations in space, neglectable friction within the fluid relative to friction between soil matrix and fluid. The general form of Darcy's equation following from this derivation is:

$$u_i = \frac{k}{\nu} \cdot g\left(\frac{\partial h}{\partial x_i} + \delta_{i3}\right)$$

with : x_i = distance in i-direction
δ_{ij} = Kronecker delta (δ_{ij}=1 for i=j and δ_{ij}=0 for i≠j)
ν = viscosity $(m^2 \cdot s^{-1})$
k = intrinsic permeability (m^2)

Hysteresis is the dependence of the retention curve upon the history of drying and wetting. Most important cause is that upon drying the pores with pore entries corresponding to a certain suction are full, whereas upon wetting these pores are, at the same soil water pressure, still empty (ink-bottle effect). Other causes are the dependence of the contact

angle between soil matrix and water on the direction of water movement (rain-drop effect), shrinkage?swelling of the soil matrix and the possible entrapment of air.

Connected to the latter are the concepts of **boundary curves** and **scanning curves**. The boundary drying curve is the retention curve obtained from the drying of a soil starting at complete saturation. The boundary wetting curve, is obtained at the wetting of an initially completely dry soil. At the same pressures this curve shows lower water contents than the boundary drying curve, due to air entrapment. Drying and wetting scanning curves are obtained by reversing the process at a point of the wetting or drying boundary curve, respectively, intermediate between saturation and complete drying. Hysteresis also influences K(h) because conductivity actually is connected to water content via $K(\theta)$, which is linked to K(h) by the non-unique function $\theta(h)$.

Navier-Stokes equation describes the combined effect of momentum balance and conservation of mass in a laminar flow of a Newtonian fluid. A Newtonian fluid is a fluid in which shear stress is proportional to the velocity gradient. The general form of the **Navier-Stokes equation** (neglecting the effect of the earth's rotation) is:

$$\frac{\partial \rho u_i}{\partial t} + u_j \frac{\partial \rho u_i}{\partial x_j} = -\left(\frac{\partial p}{\partial x_i}\right) + \nu \frac{\partial^2 \rho u_i}{\partial x_j^2} - \rho \cdot g \cdot \delta_{i3}$$

with : u_i = velocity component in i-direction
x_i = distance in i-direction
δ_{ij} = Kronecker delta ($\delta_{ij}=1$ for $i=j$ and $\delta_{ij}=0$ for $i \neq j$)

Non-uniqueness in parameter optimization means that the outcome of the parameter optimization is dependant on the initial value of the parameters.

Particle size distribution indicates the relative importance of certain particle sizes to the total volume of particles. The **particle size distribution** is said to be wide when both large, medium and small particles have an important contribution to the total volume of

particles. The **cumulative particle size distribution** has always some sort of S-shape, more or less steep, when for the particle size a logarithmic scale is used.

Pedo-transfer function is a function which relates a physical characteristic of soil or land to easier measurable quantities. The concept originally stems from quantitative land evaluation (see Bouma, 1986). In this paper the term pedo_transfer function always refers to a function which determines a retention curve from textural data.

pF, see **soil water pressure**

Pore size distribution indicates the relative importance of certain pore sizes to the total pore volume. The **pore size distribution** is said to be wide when both large, medium and small pores have an important contribution to the total pore volume. The **cumulative pore size distribution** has always some sort of S-shape, more or less steep, when for the pore-size a logarithmic scale is used.

Pressure head, see **soil water pressure**

Representative Elementary Volume (REV). Size of a domain over which averaging will yield a constant (within certain error limits) outcome, wherever the REV is placed within the medium under consideration. The concept of REV is used to pass from the microscopic the macroscopic level of description. (Bear and Bachmat, 1990). The problem of the application of this concept in soil science is that the soil is in fact no continuum, so averaging has to take place over a volume large enough to oversee individual pores.

Richard's equation describes water flow in an unsaturated porous medium. It is a combination of mass balance (continuity equation) and momentum balance (**Darcy's equation** for unsaturated flow):

$$\frac{\partial \theta}{\partial h}\cdot\frac{\partial h}{\partial t} = \frac{\partial}{\partial x_i}[K(h)(\frac{\partial h}{\partial x_i} - \delta_{i3})]$$

with : x_i = distance in i-direction

δ_{ij} = Kronecker delta (δ_{ij}=1 for i=j and δ_{ij}=0 for i≠j)

Scanning curve, see **hysteresis**

Soil water pressure is the pressure in soil water relative to atmospheric pressure. **Soil water pressure** is always equal to or smaller than zero. Assuming a constant density for the soil water, **pressure head** (h) and **suction** (ψ) are defined as $-p/(g \cdot \rho_w)$, so that these are always positive. **pF** is defined as $^{10}\log(h\ (cm))$ and is employed to compress the large range of suctions occurring under natural conditions (0-16000 cm).

Suction, see **soil water pressure**

Tortuosity is an indication of the bends in the flow path of a fluid through a porous medium. **Tortuosity** is related to the interconnectedness of successive pores. It increases at decreasing water content because more and more pores become isolated, no longer contributing to the transport of water. The rate of increase depends on the medium.

APPENDIX 1. Data set 1

Sample number	Particle size distribution													organic matter content	ρ_b	θ_s	K_s
	<0.002 mm	<0.016 mm	0.016-0.053 mm	0.053-0.075 mm	0.075-0.106 mm	0.106-0.150 mm	0.150-0.212 mm	0.212-0.300 mm	0.300-0.425 mm	0.425-0.600 mm	0.600-0.850 mm	0.850-1.190 mm	>1.190 mm				
	%	%	%	%	%	%	%	%	%	%	%	%	%	%	g.cm^{-3}	(-)	cm.hr^{-1}
A1-1	1.8	4.9	14.4	1.5	4.5	8.7	19.4	21	13.9	5.9	2.5	1.3	2	10.50	1.02	0.562	6.438
A2-1	1.4	3.5	7.5	1.5	8.3	15.9	26.2	25.9	8.1	2.2	0.6	0.1	0.2	4.19	1.39	0.427	6.408
A3-1	0.8	3.1	7.2	1.3	7.5	13.7	25.9	26.4	10.5	3.1	0.8	0.2	0.3	3.39	1.49	0.416	3.563
A4-1	0.7	2.2	5.0	0.7	2.9	8.0	35.9	30.9	9.5	3.4	1.1	0.3	0.1	3.45	1.45	0.410	58.479
A5-1	0.9	3.2	6.5	1.3	9.2	16.0	29.6	19.3	9.6	3.9	1.0	0.3	0.1	4.14	1.50	0.394	3.208
A6-1	1.9	3.5	7.3	0.6	3.9	4.7	43.3	21.5	9.5	3.5	1.3	0.3	0.6	4.80	1.31	0.453	5.313
B1-1	2.2	4.5	8.1	2.2	9.4	12.6	26.1	22.4	9.5	3.2	1.0	0.4	0.6	4.56	1.48	0.381	2.229
B2-1	1.7	3.4	5.8	1.3	6.2	11.2	22.6	37.1	9.2	2.3	0.6	0.2	0.1	4.25	1.46	0.391	2.688
B3-1	1.1	1.9	6.3	1.8	6.0	11.6	29.5	29.9	9.4	2.7	0.7	0.1	0.1	3.91	1.46	0.411	6.313
B4-1	1.9	4.1	7.3	0.2	3.8	5.4	30.4	35.7	9.8	2.7	0.5	0.1	0.0	2.39	1.53	0.372	12.040
B5-1	1.6	3.0	6.3	1.2	8.2	16.3	33.7	21.6	7.3	1.7	0.5	0.1	0.1	3.47	1.37	0.415	6.313
B6-1	1.0	2.6	6.6	1.7	7.3	11.2	29.8	27.8	9.6	2.5	0.7	0.1	0.1	4.19	1.39	0.425	6.021
C1-1	1.9	2.7	5.3	0.8	8.1	15.1	28.6	24.9	10.9	2.6	0.6	0.2	0.2	4.05	1.49	0.389	4.833
C2-1	2.1	4.4	7.6	1.4	6.7	8.7	18.3	35.5	10.9	3.5	1.4	0.6	1.0	3.90	1.45	0.428	5.188
C3-1	1.4	3.4	7.7	1.6	9.0	13.3	28.5	23.5	9.1	2.9	0.7	0.2	0.1	3.56	1.47	0.400	122.292
C4-1	2.6	3.3	0.9	0.6	8.9	19.0	29.6	21.5	10.1	3.2	1.0	0.2	0.0	1.77	1.52	0.383	8.083
C5-1	1.3	2.4	4.9	1.7	7.6	10.8	27.5	31.2	9.6	3.1	0.9	0.2	0.1	1.22	1.56	0.352	3.500
C6-1	1.9	3.9	10.9	2.9	8.1	12.8	22.9	21.1	12.0	3.4	0.8	0.2	1.0	5.85	1.23	0.506	7.083
D1-1	1.1	3.3	7.4	1.1	8.5	12.3	27.9	25.4	9.8	3.0	0.9	0.3	0.1	3.29	1.48	0.382	3.967
D2-1	1.9	3.6	6.8	2.2	9.8	16.5	30.4	19.7	7.6	2.4	0.8	0.2	0.0	2.17	1.58	0.336	3.708
D3-1	1.6	3.4	5.5	1.5	7.9	18.1	31.8	20.2	8.0	2.6	0.7	0.2	0.1	3.07	1.52	0.367	21.750
D4-1	2.3	4.9	10.9	3.6	8.1	14.8	23.7	17.4	9.7	3.5	1.1	0.8	1.5	9.09	1.18	0.531	14.771
D5-1	1.6	3.8	8.2	1.6	10.4	13.2	25.6	24.5	8.9	2.7	0.8	0.2	0.1	3.48	1.43	0.409	3.021
D6-1	2.8	3.5	9.9	3.0	10.1	16.5	26.9	16.4	7.3	2.3	0.9	0.5	2.7	5.32	1.32	0.476	4.917
E1-1	1.4	3.2	7.7	1.6	7.8	11.1	31.7	22.8	9.4	3.1	1.0	0.4	0.2	4.32	1.32	0.430	6.438
E2-1	2.5	5.2	8.3	0.6	4.8	6.2	30.2	30.8	9.1	3.1	1.1	0.3	0.3	3.95	1.44	0.399	5.813
E3-1	0.7	2.4	5.4	0.0	1.7	3.5	27.9	41.1	12.3	4.0	1.4	0.2	0.1	1.93	1.57	0.306	3.063
E4-1	2.0	4.9	7.8	1.2	10.2	13.6	27.1	25.0	7.3	2.0	0.6	0.2	0.1	3.44	1.40	0.408	8.625
E5-1	1.1	3.5	5.3	1.3	11.8	21.3	29.0	17.2	7.3	2.4	0.6	0.2	0.1	3.82	1.46	0.367	2.646
E6-1	1.6	3.8	9.2	2.2	6.9	10.4	27.0	27.6	9.4	2.5	0.6	0.1	0.3	4.59	1.46	0.419	3.621
F1-1	1.2	3.3	5.2	2.7	6.8	17.2	30.3	27.1	9.2	2.5	0.6	0.1	0.0	0.89	1.58	0.323	3.375
F2-1	0.7	2.0	4.3	2.3	8.8	16.1	31.9	23.2	8.0	2.5	0.8	0.1	0.0	0.94	1.59	0.438	33.250
F3-1	1.6	3.3	4.5	1.9	6.1	7.3	33.3	29.8	9.9	3.0	0.7	0.1	0.1	1.73	1.58	0.376	5.167
F4-1	1.2	3.2	6.3	2.0	11.9	14.2	27.2	22.8	8.6	2.6	0.8	0.2	0.2	2.12	1.59	0.355	17.208
F5-1	0.9	2.6	4.3	2.2	7.8	11.8	31.3	26.1	10.3	2.8	0.7	0.1	0.0	1.29	1.51	0.421	20.042
F6-1	2.2	5.3	8.6	2.1	10.0	12.1	30.2	20.2	8.7	2.1	0.4	0.1	0.2	3.64	1.41	0.376	?

APPENDIX 1. Data set 1 (continued)

Sample number	Particle size distribution													organic matter content	ρ_b	θ_s	K_s
	<0.002 mm	<0.016 mm	0.016-0.053 mm	0.053-0.075 mm	0.075-0.106 mm	0.106-0.150 mm	0.150-0.212 mm	0.212-0.300 mm	0.300-0.425 mm	0.425-0.600 mm	0.600-0.850 mm	0.850-1.190 mm	>1.190 mm				
	%	%	%	%	%	%	%	%	%	%	%	%	%	%	g.cm^{-3}	(-)	cm.hr^{-1}
A1-2	1.8	2.5	2.6	1.2	8.7	18.0	30.7	26.7	7.7	1.5	0.2	0.1	0.1	1.90	1.46	0.391	8.948
A2-2	1.1	3.4	7.8	1.8	8.6	13.7	29.2	22.8	8.5	2.4	0.7	0.2	0.9	4.89	1.32	0.425	2.042
A3-2	4.1	8.7	7.8	1.4	9.6	14.3	25.2	19.6	10.8	2.2	0.3	0.1	0.0	1.16	1.72	0.336	14.173
A4-2	1.1	1.1	2.1	2.8	10.7	22.6	40.4	16.9	2.8	0.5	0.1	0.0	0.0	0.93	1.51	0.444	21.354
A5-2	1.5	2.0	2.7	2.0	6.8	12.6	34.8	31.7	6.1	1.0	0.3	0.0	0.0	1.13	1.55	0.454	29.479
A6-2	1.8	2.6	7.1	1.1	6.4	10.9	21.2	20.5	15.0	8.6	4.9	1.4	0.3	4.91	1.30	0.480	46.708
B1-2	2.2	4.3	8.6	2.3	6.8	8.7	26.6	27.2	10.5	3.1	1.1	0.2	0.6	4.57	1.29	0.437	7.833
B2-2	1.1	3.4	4.8	1.1	7.8	11.5	35.8	24.7	8.0	2.3	0.5	0.1	0.0	1.94	1.39	0.390	5.240
B3-2	2.1	3.7	4.1	2.0	9.6	9.7	31.4	26.0	9.7	2.8	0.7	0.2	0.1	0.84	1.67	0.330	4.521
B4-2	1.0	1.6	3.2	1.2	11.1	20.2	30.6	22.6	7.8	1.3	0.3	0.0	0.1	1.69	1.77	0.330	8.521
B5-2	0.9	1.2	2.1	2.5	11.6	23.6	32.3	18.5	6.6	1.3	0.2	0.0	0.1	1.00	1.55	0.419	42.688
B6-2	5.8	10.5	7.6	1.9	10.7	18.2	24.1	17.1	7.8	1.8	0.2	0.0	0.1	1.85	1.41	0.398	12.356
C1-2	1.2	2.2	1.7	0.8	5.6	9.7	27.6	39.0	9.6	3.0	0.7	0.1	0.0	0.92	1.51	0.387	5.046
C2-2	1.2	1.7	4.1	2.9	12.5	18.6	26.9	20.5	9.2	2.7	0.7	0.1	0.1	0.71	1.53	0.365	9.919
C3-2	1.6	3.3	2.0	0.8	5.6	12.1	32.6	31.4	8.6	2.6	0.7	0.3	0.0	0.60	1.43	0.340	8.271
C4-2	1.1	3.2	10.7	2.3	6.6	9.6	21.0	20.6	14.0	4.9	1.0	0.3	5.8	11.18	1.10	0.518	3.302
C5-2	1.1	2.4	3.6	1.3	7.6	10.0	34.6	26.3	9.0	3.6	1.1	0.4	0.1	1.98	1.39	0.408	7.708
C6-2	1.8	2.9	5.3	6.0	21.3	20.5	24.7	12.8	4.4	1.7	0.4	0.0	0.0	1.17	1.50	0.387	2.471
D1-2	1.0	1.6	1.8	0.3	4.9	7.7	31.9	41.2	8.0	2.0	0.5	0.1	0.0	3.13	1.66	0.293	2.683
D2-2	1.0	1.6	4.8	3.2	11.0	17.7	30.9	20.3	7.4	2.2	0.6	0.2	0.1	1.20	1.61	0.340	6.604
D3-2	1.1	2.3	6.6	2.3	8.4	10.0	27.6	24.7	13.1	3.9	0.8	0.2	0.1	1.22	1.54	0.348	6.148
D4-2	1.8	2.5	3.1	0.6	6.9	10.1	24.1	35.0	10.7	4.2	2.0	0.7	0.1	0.90	1.55	0.361	13.708
D5-2	1.6	4.3	5.7	2.8	9.4	13.7	25.8	26.3	8.8	2.4	0.7	0.1	0.0	1.49	1.56	0.301	1.606
D6-2	2.7	4.8	3.9	3.0	8.4	14.9	25.1	21.5	8.6	3.5	1.4	1.3	3.6	1.39	1.58	0.359	3.729
E1-2	0.7	1.1	4.1	2.6	12.0	13.0	34.2	21.7	8.2	2.3	0.6	0.1	0.1	2.21	1.60	0.329	2.177
E2-2	0.9	2.1	3.3	0.7	7.3	13.3	27.3	32.4	9.5	2.9	0.9	0.2	0.1	1.15	1.58	0.332	3.585
E3-2	1.2	2.0	1.8	2.1	11.5	22.8	30.5	20.4	6.3	1.8	0.7	0.1	0.0	0.35	1.57	0.369	17.333
E4-2	1.7	4.2	7.0	2.6	10.1	15.3	26.4	23.1	8.2	2.0	0.5	0.2	0.4	1.78	1.52	0.402	1.513
E5-2	4.4	7.5	9.9	3.0	9.5	14.8	26.0	16.9	8.4	2.9	0.5	0.2	0.4	6.95	1.21	0.452	0.188
E6-2	1.0	1.9	3.1	2.0	10.0	12.6	30.0	26.1	11.5	2.2	0.5	0.1	0.0	2.14	1.45	0.447	18.750
F1-2	0.5	4.7	6.9	1.2	11.5	6.1	41.4	17.1	7.9	2.6	0.6	0.0	0.0	1.00	1.63	0.327	1.392
F2-2	1.3	2.5	1.7	0.5	8.8	12.6	27.8	29.6	10.8	3.9	1.4	0.3	0.1	1.08	1.59	0.332	7.521
F3-2	2.1	3.0	3.8	0.6	5.6	8.4	33.5	29.3	10.0	3.4	1.0	0.3	1.1	2.67	1.77	0.407	28.61
F4-2	1.7	2.3	4.3	2.7	9.1	13.6	28.0	25.2	8.3	3.2	1.4	0.5	1.4	1.72	1.52	0.388	8.896
F5-2	1.0	1.9	1.4	3.4	8.8	15.7	32.2	23.3	9.4	2.8	0.8	0.2	0.1	0.36	1.56	0.340	4.795
F6-2	1.1	2.8	1.8	0.7	7.9	19.6	28.5	22.5	9.2	2.3	0.6	0.1	4.0	0.96	1.62	0.446	25.375

APPENDIX 2. Data set 2 (Hopmans and Stricker, 1987)

Location		Data used in curve-fitting	α	n	θ_s	K_s
No.	Depth		cm^{-1}	-	-	$cm \cdot hr^{-1}$
1	top	retention	0.0106	1.3020	0.4151	
		retention	0.0075	1.4578	0.3901	
		retention/conductivity	0.0088	1.3723	0.4025	10.3010
	sub	retention	0.0089	2.3711	0.2915	
		retention	0.0105	1.5805	0.2676	
		retention/conductivity	0.0098	1.8508	0.2802	3.5280
2	top	retention	0.0092	1.7024	0.3776	
		retention	0.0417	1.1480	0.3803	
		retention/conductivity	0.0146	1.3461	0.3781	80.129
	sub	retention	0.0095	1.6913	0.3595	
		retention	0.0081	1.5812	0.3039	
		retention/conductivity	0.0090	1.6281	0.3318	9.9150
3	top	retention	0.0198	1.1195	0.4826	
		retention	0.0056	1.4953	0.4107	
		retention/conductivity	0.0083	1.2608	0.4463	25.461
	sub	retention	0.0344	1.3317	0.3452	
		retention	0.0433	1.3084	0.3633	
		retention/conductivity	0.0388	1.3187	0.3542	695.0
4	top	retention	0.0493	1.3202	0.3986	
		retention	0.0296	1.4331	0.3841	
		retention/conductivity	0.0377	1.3712	0.3910	96.33
	sub	retention	0.1000	1.2435	0.3972	
		retention	0.0555	1.3903	0.4107	
		retention/conductivity	0.0707	1.3122	0.4033	420.185
5	top	retention	0.0120	1.5176	0.3888	
		retention	0.0095	1.4908	0.3173	
		retention/conductivity	0.0109	1.5044	0.3529	11.03
	sub	retention	0.0386	1.2282	0.3305	
		retention	0.0256	1.8038	0.3285	
		retention/conductivity	0.0329	1.4123	0.3315	138.5
6	top	retention	0.0112	1.5673	0.4194	
		retention	0.0375	1.3011	0.3727	
		retention/conductivity	0.0196	1.3997	0.3955	31.14
	sub	retention	0.0103	2.2015	0.2973	
		retention	0.0194	1.3377	0.2963	
		retention/conductivity	0.0133	1.6260	0.2976	19.063
7	top	retention	0.0179	1.4488	0.4389	
		retention	0.0392	1.2474	0.4120	
		retention/conductivity	0.0264	1.3299	0.4263	40.062
	sub	retention	0.0242	1.3438	0.3827	
		retention	0.0119	1.5256	0.3676	
		retention/conductivity	0.0161	1.4275	0.3740	47.323

APPENDIX 3. Dimensional analysis

Dimensional analysis is a method used to separate dominant and non-dominant effects in a process. One starts with a governing equation.
For each variable (e.g. x), coefficient or constant a dimensionless variable (x^*) is introduced, expressing the ratio between the dimensional quantity (x) under consideration and corresponding reference quantity (x_c) of the same dimension and with a value that is characteristic for the process. Subsequently the original quantities are expressed as the product of the dimensionless ratio and the reference quantity ($x^* \cdot x_c$), so that each term in the governing equation becomes the product of dimensionless term and a dimensional coefficient made up of the reference quantities. By dividing all terms of the equation by one of the coefficients, one obtains the dimensionless form of the original equation. Now, by comparing the magnitudes of the coefficients before the successive terms in the equation, the relative importance of the terms and the corresponding processes can be inferred. Based on this comparison one or more terms, which are of minor importance, can be skipped from the equation, therewith simplifying the problem.

Here dimensional analysis will be applied to the derivation of Darcy's equation from the Navier-Stokes equation. In that derivation a number of dimensionless numbers occurs, namely the Reynolds number, Darcy number and the Strouhal number. The Reynolds number (Re) expresses the ratio between inertial forces (convective term in Navier-Stokes equation) and viscous forces. Re indicates the validity of a laminar approximation. The Reynolds number as it is used here does not take into account the occurrence of local spots of acceleration and deceleration, which are a result of the irregular diameter of pore channels.
The Darcy number (Da) expresses the ratio between the friction within a fluid and the microscopic friction between wall and fluid. The latter is here assumed to be proportional to velocity, viscosity and intrinsic permeability and inversely proportional to porosity (compare to Hagen-Poisseuille flow through a pipe).
The Strouhal number (St) is a dimensionless number expressing the ratio between local acceleration and convection (first and second term on left hand side in Navier-Stokes equation).
Bear and Bachmat (1990) define the Reynolds (Re), Darcy (Da) and Strouhal (St) number for saturated flow:

$$Re = \frac{V_c (k_c/n_c)^{1/2}}{\nu_c} \qquad [A3.1]$$

$$Da = \frac{k_c/n_c}{L_c^2} \qquad [A3.2]$$

$$St = \frac{L_c}{\Delta t_c V_c} \qquad [A3.3]$$

with : V_c = characteristic velocity ($m \cdot s^{-1}$)
L_c = characteristic length (m)
k_c = characteristic permeability (m^2)
n_c = characteristic porosity (-)
Δt_c = characteristic time increment (s)
ν_c = characteristic viscosity ($m^2 \cdot s^{-1}$)

The approximations underlying Darcy's equation are justified only when $St \leq 1$ and $Re \cdot Da^{1/2} < 1$ (non-stationarity is neglectable), $Re < 10$ (laminar flow) and $Da \ll 1$ (internal friction neglectable).

In the case of the one-step outflow experiment the occurrence of non-Darcian flow might be expected during the onset of the flow. The sample is still saturated at that moment so that the above mentioned dimensionless numbers can be used. At the start of the flow process the largest accelerations occur. Characteristic values for the various variables occurring in Re, Da and St are chosen as follows for the time directly after the onset of flow. V_c is estimated from measured outflow during the first 15 s, yielding $0.13 \cdot 10^{-2}$ $m \cdot s^{-1}$. L_c is taken as one-tenth of the sample height, 0.005 m. k_c was estimated to be 10^{-5} m^2, which value was calculated from a representative value for the saturated conductivity of sandy soils by $k_c = K_s \nu_c / g$. n_c was set to 0.4 and ν_c was estimated to be 10^{-6} $m^2 \cdot s^{-1}$. Finally the characteristic time-increment Δt_c is taken to be 15 s. For the dimensionless numbers this yields the following values: Re = 0.435, Da = 1, St = 0.96.
From this analysis it can be concluded that internal friction within the fluid will not cause problems of non-Darcian behaviour. But the St of almost 1 combined with $Re \cdot Da^{1/2}$ equal to 0.435 might be reason for concern. The effect of non-stationarity is not neglectable at the onset of the flow process. Also the assumption that internal friction within the fluid is neglectable compared

to friction between fluid and matrix is also not unambiguously true. However, what the effect of this non-Darcian behaviour is on the parameter optimization is not clear. Probably only the simulated outflow of the first minutes is affected and therewith only a small volume. In that case the errors become relatively unimportant, because later on the flow will obey the Darcian approximation and the error in total outflow volume becomes increasingly smaller.